# Laser-induced Breakdown Spectroscopy, Elemental Analysis

*Fang-Yu Yueh, Jagdish P. Singh, and Hansheng Zhang*

in
*Encyclopedia of Analytical Chemistry*
R.A. Meyers (Ed.)
pp. 2066–2087

# Laser-induced Breakdown Spectroscopy, Elemental Analysis

**Fang-Yu Yueh, Jagdish P. Singh, and Hansheng Zhang**
*Mississippi State University, Starkville, USA*



*Laser-induced breakdown spectroscopy (LIBS) is a laser-based technique that can provide nonintrusive, qualitative and quantitative measurement of metals in various test environments. LIBS is an emission-type technology that has been successfully applied to gas, liquid, and solid samples. The major advantages of LIBS compared to other analytical techniques is that no time-consuming sample preparation is necessary. LIBS uses the plasma generated by a high-energy laser beam to prepare and excite the sample in one step. It has the ability to perform multielement real-time analysis. Its major disadvantage is that the excitation condition is sensitive to the fluctuation of environmental conditions as well as the laser energy, which can result in poor measurement precision. The small amount of sample material used in LIBS analysis also gives poorer sensitivity for some metals compared to inductively coupled plasma atomic emission spectrometry (ICPAES) and atomic absorption spectrometry (AAS).*

*The potential of LIBS to detect toxic metals in harsh environments was recognized in the early 1970s. Recent developments towards improving its analytical capability has led to more applications. This article reviews the analytical applications of LIBS with an emphasis on environmental monitoring. A brief review of some fundamental LIBS studies is also given. The analytical abilities of LIBS are compared with some spectroscopic techniques commonly used in the laboratory, such as AAS, ICPAES, and X-ray fluorescence spectroscopy (XFS).*

## 1 INTRODUCTION

Laser-induced breakdown phenomena were observed just after the invention of the laser in 1963. Initial work was focused on understanding the various mechanisms involved in the process. As the material is atomized and excited at the high temperature of laser spark plasma, the potential for using LIBS for elemental analysis was soon recognized by many researchers. The application of LIBS to gases, liquid, and solid samples was explored by various groups from 1970 to 1985. Compared to other analytical techniques, LIBS uses very small amounts of samples, and no sample preparation is necessary. It has the ability to perform real-time analysis because it prepares and excites the sample in one step. The disadvantage of LIBS is that the plasma condition varies with the environmental condition as well as laser energy fluctuation, resulting in poor measurement precision. The microgram-sized samples used in LIBS also causes lower sensitivity for some elements. Since the late 1980s, many studies on LIBS characteristics for quantitative measurements have been initiated. Techniques to improve the precision and sensitivity of LIBS are also being tested This ongoing development has improved the analytical capabilities of LIBS and led to more applications.

The application of LIBS to environmental monitoring has drawn significant attention. LIBS has been used to detect toxic metals in soil and paint, and has been explored as a multimetal continuous emission monitor (CEM). There are a few reports on the application of LIBS to detect radioactive species. LIBS has also being used to measure the composition of molten metals and glasses. This article reviews the application of LIBS to analytical problems with an emphasis on environmental applications. Detailed reviews on the LIBS principle and other

*Encyclopedia of Analytical Chemistry*

applications can be found.[1-5] Brief reviews of some fundamental and experimental application of LIBS are given in sections 2 and 3 of this article. Environmental monitoring applications are discussed in section 4. LIBS's quantitative capability is addressed in section 5. A brief discussion of future developments is given in the last section.

## 2 FUNDAMENTAL STUDIES

The physics of laser-induced breakdown has been studied extensively.[6,7] The minimum optical power density required to form a plasma is called the breakdown threshold; different types of laser, sample, and ambient conditions will have different breakdown thresholds. A laser power density greater than $10^{10}$ W cm$^{-2}$ is generally required to generate a breakdown in air using a Q-switched Nd : YAG laser of 10–15 ns duration. Breakdown thresholds of solids and liquids are usually much lower than for gases. Table 1 lists some measured breakdown thresholds in different media.[8-11]

The two mechanisms responsible for electron generation and for growth in laser-induced breakdown are multiphoton absorption and collision-induced ionization. Multiphoton absorption involves simultaneous absorption of a certain number of photons by an atom or molecule, to cause its ionization. This mechanism produces the initial few free electrons in the focal volume. The electron density grows linearly with time. Generally, this mechanism is not the major process in the growth of electrons in laser plasma. It is more important for a short-wavelength laser ($\lambda < 1\,\mu$m) or low density ($P < 10$ torr in $N_2$).[12] In the collision-induced ionization process, free electrons in the focal volume are accelerated by the electric field of the laser and gain energy by colliding with neutral atoms. After the electrons have gained sufficient energy, they can ionize atoms by collision and this causes the electron density to grow exponentially with time. This process is dominant at high pressure ($P > 100$ torr in $N_2$) and long wavelength ($\lambda > 1\,\mu$m).[12] The breakdown threshold in this process has a $\lambda^{-2}$ or $\lambda^{-3}$ dependence.[12]

**Table 1** Breakdown thresholds for various media

| Test medium | Laser type | |
|---|---|---|
| | Ruby (0.69 μm) ($10^{10}$ W cm$^{-2}$) | $Nd^{+3}$ (1.06 μm) ($10^{10}$ W cm$^{-2}$) |
| Gas[a] | | |
| Air | 20 | 7 |
| Ar | 8 | 2 |
| He | 15 | 4 |
| $N_2$ | 21 | 9 |
| Liquid | | |
| Tap water[b] | 3.8 | 10 |
| Distilled water[c] | | 62 |
| Benzene[c] | | 4.4 |
| Solid[d] | | |
| NaCl | 15 | 14 |
| KBr | 5.7 | 5 |

[a] Pressure = 1 atm; ruby, $T_p = 40$ ns; $Nd^{3+}$, $T_p = 40$ ns.[8]
[b] Ruby, $T_p = 21$ ns, $Nd^{3+}$, $T_p = 50$ ns.[9]
[c] $Nd^{3+}$, $T_p = 50$ ns.[10]
[d] Ruby, $T_p = 10$ ns; $Nd^{3+}$, $T_p = 10$ ns.[11]
$T_p$ is the laser pulse width.

The characterization of laser-induced plasma (LIP) has been carried out both in time and spatial evolution of the plasma. The evolution of laser plasma can be divided into several transient phases. The initial plasma (0–100 ns) is characterized by high electron and ion densities ($10^{17}$–$10^{20}$ cm$^{-3}$), and temperatures around 20 000 K. The emission spectrum from the early stage of the plasma is characterized by a continuum background emission due to bremsstrahlung (strong collisions between the free electrons and the excited atoms and ions) and recombination of electrons with ions processes in the plasma. Emission lines from ions and atoms can be found after about 300 ns delay. These lines are superimposed on the strong continuum background. Owing to the high electron density, the emission lines are broadened by the Stark effect. As the plasma expands and cools, the electrons and ions recombine, and a characteristic loud sound can be heard due to the shock wave emitted from the plasma. The continuum background decays rapidly and the atomic emission lines become narrower and weaker. After the initial plasma (>10 μs), the atomic emission decays slowly, and emission from the simple molecule appears. Figure 1 shows LIBS spectra recorded at delay times of 0.25, 5, and 35 μs. As shown in the figure, a properly selected detection window can improve the signal-to-background ratio ($S/B$) of the data, which is very important to quantitative measurement.

The excitation characteristics of the laser plasma are determined by the plasma properties, which can be described by the temperature and electron density of the plasma. The analytical measurements are generally performed after the initial plasma, when a state of local thermal equilibrium (LTE) is achieved. At the LTE condition, the analyte intensity is proportional to the relative population of the level, and follows the Boltzmann distribution. The Griem criterion (Equation 1) is usually used to check the existence of LTE in a laser plasma[13]

$$N_e(\text{cm}^{-3}) \gg 30\,545 \times 10^{17} \times T_e(\text{K})^{1/2} \times \left(\frac{Z^2}{\lambda(\text{nm})}\right)^3 \quad (1)$$

where $N_e$, $Z$, and $\lambda$ are the critical electron density for LTE, the degree of ionization, and the transition wavelength, respectively.

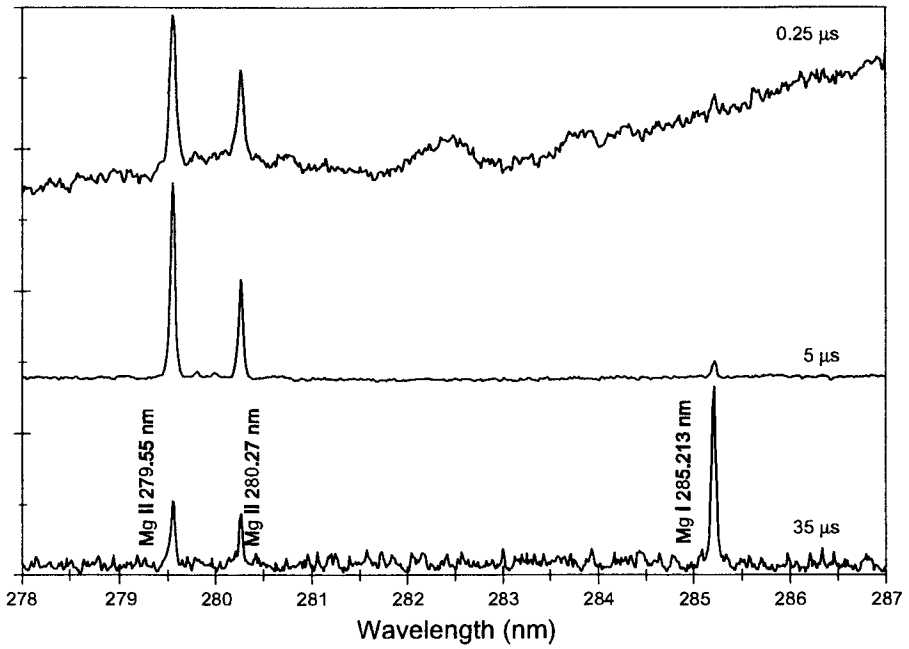


**Figure 1** LIBS spectra recorded at different delay times.

Under LTE, the intensity of an emission line at $\nu_{ji}$ can be expressed (Equation 2) as

$$I_{ji} = n(h\nu_{ji})\frac{A_{ji}g_j}{Q(T)}\,e^{-hcE_j/kT} \qquad (2)$$

Here, $n$ is the total number density of a neutral or ion of the element, $g_j$ is the statistical weight of the excited state, $A_{ji}$ is the transition probability, $E_j$ is the energy of the excited state in units of $cm^{-1}$, $h$ is Planck's constant, $k$ is the Boltzmann constant, $T$ is the plasma temperature, and $Q(T)$ is the partition function.

The details of LIP are described elsewhere. Here, only the characteristic and physics parameters are discussed, which are important to quantitative analysis of LIBS. At present, the physics of LIP is not fully understood but work in this area continues.

### 2.1 Effect of Physical Variables

Variables that can influence LIBS measurements are laser properties (i.e. wavelength, energy, pulse duration and shot-to-shot power fluctuation), focusing spot size, ambient conditions, physical properties of the sample, and the detection window (delay time, gate width). How these parameters affect the precision and accuracy of LIBS are addressed below.

#### *2.1.1 Laser Parameters*

In LIBS, a high-energy laser beam is used to form a plasma to prepare and excite the sample. As the laser plasma is the excitation source of the LIBS measurement, the properties of the laser can influence the analytical qualities of the LIBS measurement. Regardless of the type of laser used, a power density of the order of $10^9\,W\,cm^{-2}$ is required. If the laser energy is very close to the breakdown threshold, the pulse-to-pulse fluctuation can cause the plasma condition to be unreproducible, which results in poor measurement precision. The LIBS signal is proportional to the laser energy while the laser plasma is in the optical thin region. Figure 2 shows the dependence of the analyte line intensity and background on laser energy. When the laser energy further increases, it produces a very dense and hot plasma that can absorb laser energy and cause self-absorption. This will lead to an increase in the continuum emission and a decrease in the signal intensity. Laser wavelength can also affect the plasma-formation process. Collision-induced ionization is the dominant process for LIP with a long-wavelength laser. As the laser wavelength decreases, the collision-induced ionization rate decreases, and the multiphoton process increases. A maximum breakdown threshold is found in the intermediate laser wavelength. Laser wavelength can also affect energy coupling between the laser and the sample. Studies have shown that the use of an ultraviolet (UV) wavelength can improve the energy

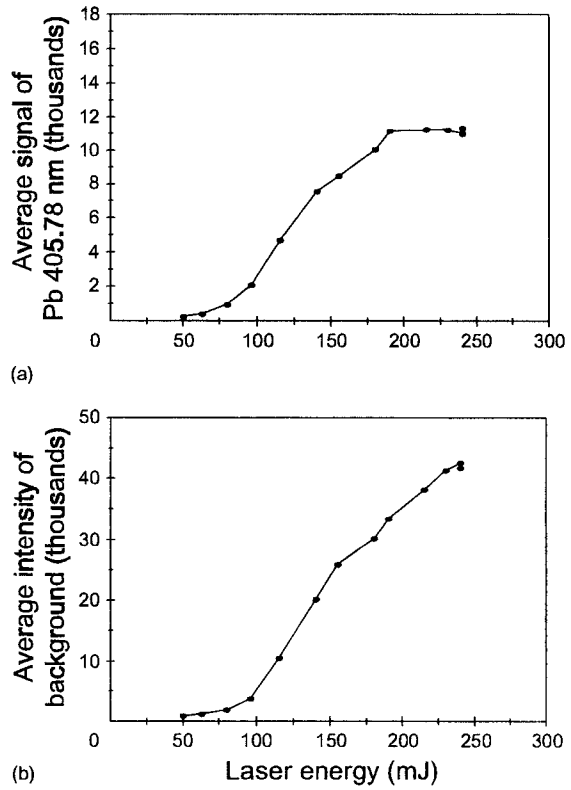


**Figure 2** Dependences on the laser energy of (a) the LIBS signal and (b) the background intensity.

coupling efficiency due to its low reflectivity for most metals.[14]

Studies of laser wavelength on material removal from the sample surface have been performed by many researchers.[15,16] Dahmain[17] has also derived the mass-ablation rate with absorbed laser intensity $I_a$, laser wavelength $\lambda$, and atomic number $Z$ based on experimental data for a laser energy lower than $10^{13}$ W cm$^{-2}$ and $Z \leq 13$ (Equation 3):

$$m(\text{kg s}^{-1}\,\text{cm}^{-2}) = 65\left(\frac{I_a\,\text{W cm}^{-2}}{10^{13}}\right)^{5/9} \lambda^{-4/9}(\mu\text{m})Z^{1/4} \quad (3)$$

Besides laser wavelength and laser energy, the laser pulse duration and laser shot-to-shot fluctuation can also affect the signal reproducibility and, hence, LIBS precision. When the laser duration is short compared to electron energy loss time, multiphoton absorption dominates over collision-induced ionization. A study has shown that the threshold intensity increases with decreasing laser pulse duration for laser pulses shorter than $10^{-7}$ s at atmospheric pressure.[18] A 1000-fold higher breakdown threshold was found with an Nd:glass laser of about 10 ps than for a nanosecond width pulse in atmospheric air.[19]

### 2.1.2 *Physical Properties of the Sample*

All types of material can be sampled using LIBS. However, the physical properties (such as reflectivity of the sample surface, density, specific heat, and boiling point of the target) can have a considerable influence on the result. The surface reflectivity determines the fraction of the laser energy that can be absorbed by a sample, and hence that can affect the material ablation rate. Study has shown that if the laser energy is high enough, the laser energy can still effectively couple to a sample with high reflectivity. This is because, during a laser pulse, the laser energy causes rapid heating of the sample and this results in a sample phase change which significantly reduces the reflectivity.

The laser plasma heats the sample to cause the vaporization and atomization of the sample material. The amount of material vaporized depends on thermal properties of the sample (i.e. conductivity, specific heat, and boiling point). At a low laser power densities, thermal conductivity is the most important parameter for material vaporization. If the material has a high thermal conductivity, the absorbed heat is conducted away quickly and results in a lower amount of material being vaporized. At higher laser power densities, the heat provided is too quickly to be conducted away; therefore, the latent heat of vaporization of the sample becomes a more important factor in determining the amount of material vaporized during a laser pulse.

### 2.1.3 *Focal Properties*

High laser power densities can produce a LIP which has higher excitation temperatures with minimum matrix interferences due to more complete atomization. It is a condition preferable to quantitative measurement. The laser power density at the focal volume is inversely proportional to the focused spot size. For a laser beam with a Gaussian profile, the focused beam waist ($w_0$) is given by Equation (4)

$$w_0 = \frac{\lambda f}{\pi D} \quad (4)$$

where $D$ is the radius of the unfocused beam, $f$ is the focal length of the lens, and $\lambda$ is the laser wavelength. A higher laser power density at the focal point can be achieved by reducing the focused beam waist using a shorter focal length lens or larger unfocused beam.

Effects of the laser-spot diameter on the sample ablation rates were studied by Wolff-Rottke et al.[20] They found the ablation rate increased with decreasing

spot diameter in the range 10–200 μm for a pulse laser. However, if the size of the spark is very small and the distribution of material within it is inhomogeneous, the precision and accuracy of the measurement is degraded.

A short focal length lens is preferred to produce a highly localized spark for a spatially resolved measurement. A long focal length lens provides a larger focal volume and is usually used when the focal lens cannot be kept close to the sample. This situation requires higher laser energy to produce the laser spark, and the larger focal volume associated with the long focal length can cause particle-induced sparks – formed at different locations along the focal axis – and this introduces noise into measurements.

The lens-to-surface distance (LTSD) is a critical parameter for the LIBS measurement of a solid sample. If the laser beam is tightly focused on the surface, a change of the LTSD of a few millimeters can affect the absolute analyte intensity. Studies have shown that by defocusing the laser beam on the sample surface a more reproducible LIBS signal can be obtained.[21] Therefore, this technique can be used to improve LIBS precision.

### *2.1.4 Detection Time Window*

In LIBS, the desired atomic emission signal is always accompanied by a strong continuum background. As the continuum background and analyte signal decay with different rates, it is possible to use a time-resolved technique to discriminate against the strong continuum radiation and also avoid spectral interference between species that emit at different times during the plasma decay (see Figure 1). The detection window is selected to obtain an optimum *S/B*. As the background signal decays at a faster rate than the emission signal, the best *S/B* can be achieved at a long delay time. The long delay time also ensures that LTE is achieved. Generally, signal-to-noise ratio (*S/N*) and *S/B* values follow the same trend as the delay time changes. However, a low *S/B* can sometimes give a good *S/N*. Therefore, the selection of the best detection window should depend on both *S/B* and *S/N*.

### *2.1.5 Ambient Conditions*

The hot plasma interacts with the surrounding gas by expanding the high-pressure vapor, driving a shock wave into the atmosphere and transferring the energy to the atmosphere via heat transfer and heating by the shock wave. The size and shape of the LIP are largely dependent on the ambient conditions such as pressure, gas composition, mass density of the gas, etc. The breakdown threshold of gas near atmospheric pressure ($10^2$–$10^3$ torr) has been examined.[6] A pressure dependence of $P^{-m}$, where $m$ is close to 1, was found for pulse widths of 10–100 ns. This is consistent with the electron atom collision frequency's dependence on pressure. Kuzuya et al. have taken plasma images at different pressures.[22] They found that the spatial confinement of the plasma becomes stronger with increasing gas pressure. The confining effect produces a denser and hotter plasma which could cause an increase in both the emission period and the emission intensity. At low pressures, owing to the weak confining effect of the plasma by the surrounding gas, the laser-produced plasma expands rapidly and becomes thin, resulting in a decrease in the emission intensity. At moderately high pressures, high-temperature and high-density plasma is generated, and the intensity of the continuous emission spectrum is very high; also, the self-absorption effect takes place to a remarkable extent due to the increase in concentration of the absorbing species surrounding the hot plasma. As a result, one is faced with difficulty in terms of precision and sensitivity. To obtain intense emission spectra free from self-absorption, LIBS measurements should be performed at a moderate pressure range ($50 < P < 500$ torr in air).

The effects of various atmospheres including Ar, air, $O_2$, $N_2$, He on LIBS spectra have been studied.[22,23] The inert gas acts like a buffer gas to prevent rapid oxidation of the free atom in the plasma. Argon breakdown occurred in the plasma at a relatively high pressure. The argon atmosphere can enhance the analytical signal by re-excitation of atoms, resulting from collision with photon-excited argon. LIP in the Ar atmosphere has a higher plasma temperature and longer emission period due to the low thermal conductivity of Ar. The higher plasma temperature in the Ar atmosphere also produces the highest continuum background. The emission characteristics of LIP from the air atmosphere are similar to that from the Ar atmosphere. However, the continuum background is only half of that in the Ar atmosphere. Helium has higher thermal conductivity and higher ionization potential than nitrogen or argon. Hence, it has a high-energy coupling efficiency compared with Ar or air. Therefore, background from a He atmosphere is lower and less sensitive to changes in laser energy and pressure.

## 2.2 Analytical Characteristics

In LIBS, the material in the laser spark is immediately reduced to elemental form, and the resulting atoms are electronically excited due to the high plasma temperature. The characteristic atomic and ionic emissions from the excited species are detected and used for analysis. Owing to the rapid expansion and the subsequent cooling effect, the analytical signal from a laser plasma is time dependent. In the first several microseconds, the continuum background emission dominates. As the plasma cools down, the background emission decreases

significantly and ionic and atomic line signals become the dominant spectral feature. Most LIBS work is performed with time-resolved measurements to avoid the strong continuum background in the initial plasma and to improve the *S/B*. Kagawa and Yokoi found that the LIP consists of two distinct regions when using an $N_2$ laser (337.1 nm) – primary plasma acts as an initial explosion energy source and emits an intense continuous emission background for a short time just above the surface of the target; secondary plasma expands with time around the primary plasma.[24] It is formed by excitation from the shock wave and by emitting sharp atomic emission lines with a low background signal. The shock wave travels in the opposite direction of the laser beam, to heat and ionize the gas it passes through. The gas is then more capable of absorbing laser radiation and becomes the heat source to maintain the shock wave in the initial stage. Studies have shown that emissions from secondary plasma are suitable for quantitative analysis. Several researchers have proposed the use of time-integrated LIBS in the secondary plasma for quantitative elemental measurement. Time-integrated LIBS does not require the expensive gated detection system necessary in time-resolved LIBS. Therefore, the cost of the LIBS system can be greatly reduced.

The theoretical analysis of emission lines assumes LTE in the environment. Assuming LTE, the plasma temperature and electron density can be used to understand the atomization, ionization, and excitation processes occurring in the plasma. The plasma temperature can be determined from Equation (2) using the relative intensity of two lines of a given atomic species. If more than two lines of intensities are available, the temperature can also be extracted through the Boltzmann plot method.[25] The concentration ratio can be determined from the intensity of the analytical lines free from spectral interference. For this measurement, analyte lines with similar upper energies should be chosen to compensate for changes in the plasma. The degree of ionization for different elements can be quite large, therefore the degree of ionization will also need to be considered in the calculation of the concentration ratio.

The interaction of the laser pulse with the sample strongly influences plasma properties. In a gas, most laser energy is used to excite the sample. But in liquids and solids a lot of laser energy goes into material vaporization and less energy is left for excitation. Therefore, the optimum experimental conditions for different samples will be different. Some characteristics of LIBS in different phases of samples are discussed below.

### *2.2.1 Solid Sample*

Both conducting and nonconducting solid samples can be analyzed with LIBS. As the laser beam is focused on the sample surface, the sample material absorbs the laser energy to melt and vaporize the target material. The vapor absorbs more energy and forms a high temperature plasma near the surface. The plasma expands into the atmosphere and transfers its energy to the atmosphere. Highly ionized emission lines can be found close to the target surface, whereas singlely ionized and neutral emissions appear further away from the surface. As the laser breakdown threshold is lower in solids than in gas, generally less laser energy is needed for solid-sample measurement. The analyte signal is proportional to the laser energy. Increasing the laser energy could cause ambient gas breakdown prior to the formation of metal vapor plasma. This will influence the laser energy coupling to the target and result in a weak analyte signal, because laser energy is used to vaporize and excite the sample rather than to produce air breakdown. A lower plasma temperature is expected for solid-sample measurement. The short-wavelength laser seems to give a greater ablated mass and better *S/B*. Study has also shown that the relatively colder plasma generated with a short-wavelength laser can result in incomplete atomization and, hence, a poorer analytical result.[26] The interaction of the laser spark with the sample surface causes nanograms of material to be ablated from the surface and form a small crater on the sample surface. The size of the crater is independent of the sample material, but the depth of the crater depends on the type of matrix[27] and is proportional to the thermal conductivity of the sample material.

Hwang et al. used an ArF excimer laser to study laser energy with emission intensity for four metals (Cu, Zn, Ni alloy, and iron alloy).[28] They compared the experimental data with calculated mass removal $m(t)$ which was derived based on a heat conduction mechanism (Equation 5):

$$m(t) = AIt + BI^2t^{3/2} \tag{5}$$

where $I$ is the laser irradiance and $A$ and $B$ are the constants determined by the thermal properties of the metal.

Good correlation between the experimentally obtained emission intensity and theoretically calculated mass using the above equation was found for the four metals studied. Experiment shows that the LIBS signal also changes with time when the same location is sampled by the laser pulse (Figure 3). As the laser continuously samples at the same location, the crater size changes and results in a time-varied LIBS signal. To obtain reproducible results, LIBS measurements should be taken after a certain ablation time when the signal is at a more stable level. If possible, the sample should also be slowly translated to ensure that the measurement is performed at a new spot each time.

Surface properties can affect the material ablated from the sample, and therefore can affect LIBS precision and

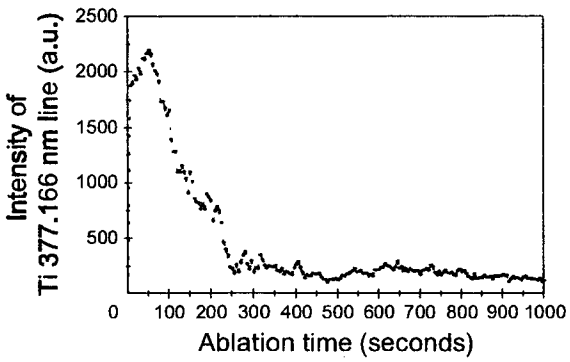


**Figure 3** Dependence of the LIBS signal on the ablation time.

accuracy. As the laser spark only interacts with the sample surface, a clean surface that has the representative elements of the bulk sample is necessary. Surface contamination can greatly distort LIBS analysis. However, this problem can be solved by applying a few laser shots at the same spot to clean the sample surface, so that reliable LIBS signal can then be obtained. Sample homogeneity is very important for bulk analysis. For an inhomogeneous sample, averaging the data taken at various locations of the sample can improve the accuracy of the measurement. The sample roughness can change the lens-to-sample distance from shot to shot and, therefore, influence the plasma characteristics and also affect the LIBS precision. Therefore, choosing a smooth surface for LIBS analysis can also improve LIBS precision.

The presence of a buffer gas also affects the energy coupling to the target and, hence, the LIBS signal. Some spectral interference can also be deduced with the selected buffer gas. For example, the interference of C emission due to the dissociation of CO or $CO_2$ in air can affect the accuracy of carbon measurement in molten steel. Use of an Ar atmosphere can improve the C detection and minimize the interference from air atmosphere. At 1 atm, a high density and high temperature plasma is generated, emitting a strong continuum emission, and self-absorption takes place. This reduces the system sensitivity and the linearity of the calibration curve. One way to improve the detection sensitivity is to use gated detection. The other method is to reduce the pressure of the buffer gas. Lee et al. found the emission characteristics generated by different sample species were quite different.[29] For spectrochemical analysis, different detection windows are sometimes needed for different metals.[29]

Castle et al. conducted experiments to find the parameters which can be used to improve LIBS repeatability for solid samples.[30] The variables considered important to solids analysis are laser energy, degree of focusing, sample translation speed, buffer gas, surface contamination, and surface smoothness. They found the sample translation velocity, laser pulse energy, and the number of spectra averaged to be the most important factors to improve LIBS precision. Parameters such as gate delay, surface roughness, and background correction have the least effect on LIBS measurement precision.

### 2.2.2 *Liquid Samples*

The physical properties of the laser spark in liquids have been studied extensively.[31] The application of LIBS in liquid analysis was not demonstrated until 1984.[32] LIBS for liquid-phase analysis can be performed by focusing the laser beam in the bulk liquid or at the surface. Bulk liquid analysis does not require a stable free surface. It avoids the liquid splashing due to the plasma shock wave propagated through the liquid surface which can cause the contamination of the optical components and shot-to-shot signal fluctuation. However, it requires a liquid that is transparent at the wavelength of the laser and the analyte line. When plasma forms inside a liquid, the atomic and ionic emissions from the constituent elements have relatively short lifetimes compared to the spark in air. Also, emissions from the background continuum, neutral and ionized atoms, and simple molecules appear simultaneously. Therefore, the time-resolved measurement cannot effectively eliminate spectral interferences for liquid analysis. However, a significant improvement of *S/B* for liquid analysis has been demonstrated with a shorter laser wavelength.[33] Studies of the effect of laser wavelength on the analysis of liquid using LIBS found that a 532 nm laser beam produced a very strong continuum background interfering with the analyte signal, whereas a 193 nm laser beam produced several orders of magnitude higher analyte signal with a relatively dimmer plasma. The improvement on *S/B* with a short-wavelength laser is because the LIP process became less thermal, and the optical energy is effectively coupled into the target rather than heating up the plasma shield. This avoids violent ablation while the liquid is absorbing the laser energy, and makes single-shot measurement in liquids possible.

The LIBS detection limit in liquids is only sufficient for measurement of the minor and major species. To improve the LIBS detection limit in liquids, several techniques were tested. A technique utilizing two sequential laser pulses to sample the same volume of liquid has shown significant improvements in the detection limits of some elements in liquids. The two sparks are spatially overlapped and temporally separated. The first spark vaporizes the liquid, producing a gaseous cavity containing species characteristic of the liquid. The second spark excites the vaporized material. The detection limit for boron had been improved 15 times by using the sequential spark method.[32] However, the sensitivity of Li and

Na did not change with this double spark technique, and it is believed that these elements are fully excited by the single spark.

The detection limits of some elements were improved by forming the laser spark on the surface of the liquid, which produced a higher-temperature spark than the spark formed in the bulk liquid. Uranium could be detected in the bulk liquid at $300\,g\,L^{-1}$, whereas a detection limit of $0.1\,g\,L^{-1}$ can be achieved with the surface excitation technique.[34]

For LIBS measurements in liquids, it is also useful to send the laser beam through the side or the bottom of the mixture, to avoid optical interference from liquid splashing and the gas bubbles liberated as the liquid–gas surface.[32] Long spectral averaging should be used to improve LIBS shot-to-shot fluctuation in liquid application.

### *2.2.3 Gas Samples*

LIP in gas has been studied extensively.[6] The breakdown in the atmospheric pressure gases were in the cascade ionization mechanism where the threshold was proportional to the ionization potential of the gas and inversely proportional to the collision frequency. The laser breakdown threshold depends on laser wavelength, gas pressure, and laser energy. The experimentally obtained breakdown threshold is much less than that predicted by theory, because the presence of aerosols causes aerosol-induced breakdown. The mechanism of aerosol breakdown is not fully understood, but experimental data shows that aerosols, acting as seeds, can significantly lower the breakdown threshold of clean gas. Smith and Brown have shown that aerosol-induced breakdown has a strong dependence on gas species, pressure, and laser wavelength, similar to that predicted for a collision-induced process.[35] They also demonstrated that, in the presence of micron-sized aerosols and impurity particles, the breakdown threshold in a gas is inversely proportional to the size of the focused laser beam. This is because the probability of finding a particle of sufficient size within the focal volume is higher.

Typically, laser-induced air breakdown has a plasma temperature of 20 000 K and an electron density of $10^{17}$–$10^{18}\,cm^{-3}$ after the plasma is formed. Emission from CN can be observed from LIP in air. The CN is produced from the reaction between C and N, produced in the spark. The intensity of the CN bands depends on the concentration of a C-containing compound in the gas stream. The elements in the spectral region covered by the CN bond have less sensitivity due to this spectral interference.

LIBS can directly measure a gas sample, eliminating the need of sample preparation. Cremers and Radziemski detected Cl and F in air with detection limits of 80 ng and 2000 ng respectively.[36] They found that the absolute detection limit for Cl and F can be improved to 3 ng in an He atmosphere. Radziemski et al. used LIBS to detect Be, Na, P, As, and Hg in air.[37] Owing to the small sample volume and possible sample inhomogeneity, the measurement precision in a gas sample is generally poor. Variously sized particulates in the gas can cause breakdown to occur at different locations along the axis of the laser beam, and this leads to significant signal variation. The variables affecting the characteristics of LIBS spectra in a gas include particle size, gas pressure, temperature, and laser energy. For quantitative measurements, the calibration procedure should keep these variables as close to the measurement conditions as possible.

## 2.3 Interference

Three types of interferences – self-absorption, spectral overlap (spectral line interference, band interference), and matrix effect (chemical interferences) – are generally encountered in LIBS. Self-absorption occurs when the emission from the hotter region is absorbed by cool atoms surrounded by the high-temperature core of the laser plasma. To avoid the problems with self-absorption, resonance lines should only be used for the measurement of trace elements.

Spectral interference due to line overlap is very common, because the resolution depends upon the monochromator used. Care should be taken to avoid spectral interference lines in the analysis. Emission lines are often superimposed on bands emitted by oxides and other molecular species from air or samples. A background correction for band emission is necessary. The absolute intensity of an analyte line can be obtained by subtracting the peak height from the background signal near the analyte line.

The physical and chemical properties of the sample can affect the plasma composition, a phenomenon known as the matrix effect. The matrix effect can result in the sample being ablated differently from the target sample. This was found in measurements of Zn–Cu alloy foil, for which the Zn/Cu weight ratio was found to be as much as 30% greater than that of the sample (independent of the laser energy, number of laser pulses, and linear to the weight ratio of the sample).[4] The matrix effect may be due to the incomplete vaporization (atomization) in LIP. Some researchers suggest including a correction factor in the calibration to take into account the matrix effect.

Sometimes interferences from the same element, dissociated from the molecular species in the atmosphere, can cause a higher inferred concentration. In carbon measurement in air, atmospheric $CO_2$ near the laser

spark is dissociated, and the resulting carbon atoms are added to those arising from the sample. This leads to a higher inferred carbon concentration. To improve the carbon measurement, LIBS has to be performed in a $CO_2$-free environment. Aguilera et al. have shown that, for carbon measurement in steel, a nitrogen environment effectively eliminates the residual carbon emission.[38]

Other types of interference include signal fluctuations due to particles and detector saturation by a very intense signal. In addition to experimental precaution, certain data selection schematics are sometimes needed to exclude some distorted data. The resonances lines are not often the most suitable lines for quantitative analysis, because they are susceptible to self-absorption. Reducing the pressure of the surrounding atmosphere can minimize the occurrence of self-reversed emission.

As the plasma condition fluctuates from pulse to pulse, and it is difficult to control the variables associated with the excitation condition, an internal standard is generally employed to compensate for the effects of laser plasma variation. An internal standard is a major element in the sample. The concentration of the internal standard is known and always the same. An emission line of the internal standard is selected for measuring the relative concentration of the other elements in the samples using the intensity ratio of the analyte line to the standard line. The internal standard line is chosen so that the excitation energies and partition functions of the analyte and internal standard lines are similarly matched, so as to compensate for changes in the plasma. To minimize the effects of the spectral response of the detection system at different spectral regions, the analyte lines and the standard line should be chosen from the same spectral region. The matrix effect, which causes the sample to be ablated differently from the target sample, cannot be corrected with the internal standard. The requirements to perform a matrix-independent measurement by using internal standard are: complete atomization of particles and droplets in an LTE microplasma; and the intensity ratios of line pairs of different elements with approximately the same excitation energies must be dependent only on the concentration ratios in different matrices.

## 3 EXPERIMENTAL TECHNIQUES

### 3.1 Experimental Methods

Since the first report of a laser-induced spark with a ruby laser by Maker, Terhune, and Savage in 1963,[39] a variety of experimental methods have been developed to perform basic research and practical applications. The development of LIBS is closely related to the development of laser techniques. From the early ruby and $CO_2$ lasers to more recently and widely used Nd:YAG and excimer lasers, more powerful, reliable, and compact laser systems have been used to perform LIBS. LIBS development is also based on the development of detectors, fiber optics, and computer technology. New detectors such as the intensified charge coupled device (ICCD) have replaced the old photomultiplier tube (PMT) and photodiode array, and have achieved much faster time responses and higher *S/N* values. Recent computer technology advances have enabled LIBS to perform real-time operations, which have enhanced its capability as a method for process monitor and control.

In 1982, Sandia National Laboratories-Livermore reported a time-integrated LIBS system for combustion applications with a Q-switched $CO_2$ transversely excited atmospheric pressure (TEA) laser.[40] The laser generates a series of mode-locked pulses separated by 7.8 ns extending over about 1 μs with total energy about 1 J at a wavelength of 10.5 μm. The beam is expanded, then focused at the point of interest. The emission from the induced spark is collected in the direction perpendicular to the beam and coupled to a 1 m spectrometer with proper optics. An intensified diode array was used to record the LIBS spectrum.

Almost at the same time, L.J. Radziemski et al. introduced a time-resolved technique to record the LIBS signal.[37,41,42] As the emission characteristics of the induced spark vary with time, the time-resolved measurement can temporally separate the emissions from different species in the induced plasma. This technique has been successfully used to maximize the *S/B* and to minimize the spectral interferences between atoms of different ionization stages as well as between atoms and molecules. In the time-resolved detection, the detector was only exposed to light during a specified gate time which is controlled by a time gate pulser. The gate pulse signal was delayed with respect to the laser pulse with a width of 200 ns to several μs. It provides a high voltage to the detector intensifier to only record the signal during the time of the gate. Figure 4 is a diagram of their system for time-resolved LIBS measurement.[37] An Nd:YAG laser operated at 1.064 μm (pulse width 10 ns and pulse energy 100–300 mJ) was used to generate the laser spark. The array detector, consisting of 1024 diodes in 25.4 mm, was controlled by a multichannel analyzer to record LIBS spectra. The sample was delivered by a nebulizer/heat-chamber system into a six-armed crossed-sample chamber where the laser beam, observation direction, and the sample flow are perpendicular to each other. With a different gate time, the ionic and neutral lines of nitrogen were successfully observed. This time-resolved technique was later adopted by many researchers due to its ability to obtain a better *S/B*.

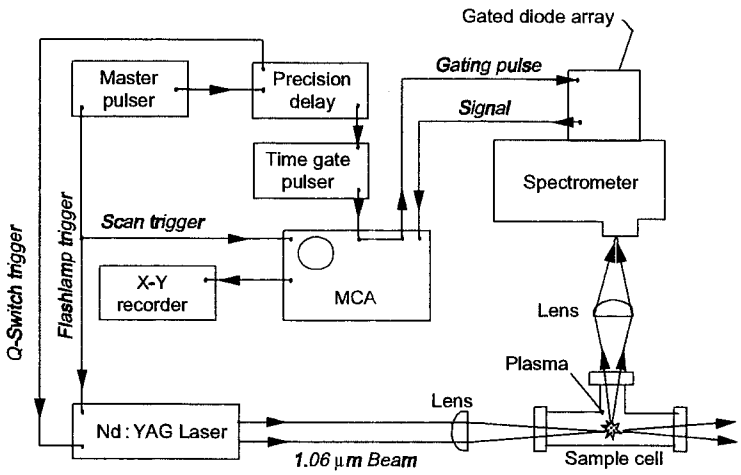


**Figure 4** Diagram of the time gated diode array system for LIBS measurement. (Reprinted from L.J. Radziemski, T.R. Loree, D.A. Cremers, N.M. Hoffman,[37] Copyright (1983) American Chemical Society.)

In 1984, D.A. Cremers et al. reported two experimental methods for LIBS measurements of liquids.[32] The two methods are repetitive single spark (RSS) and repetitive spark pair (RSP). In RSS, an Nd:YAG laser operated at 1.064 μm was focused into the liquid by a pair of 5 cm focal length lenses. The beam was focused into the cell through a quartz window on the bottom side. The cell was constructed of Teflon® and its volume was 20 $cm^3$. A small, intense, reproducible spark was obtained when the beam was focused in the liquid very close to the input window (within 2–5 mm). A strong pressure generated by the spark was observed. The spark light was collected at right angles to the laser beam. Either a PMT with boxcar averager or a photodiode array with multichannel analyzer was used. The signal was temporally resolved and averaged over many shots. In RSP, two Nd:YAG lasers were employed to generate a pair of sparks separated in time by about 18 μs. The beams from the two lasers were spatially superimposed with a 50%T:50%R beam splitter (R = reflection and T = transmission). The second spark is generated inside the gaseous cavity formed after the first spark. The signal intensity of some species was found to be enhanced significantly with the RSP method.

The RSP technique was applied to solid samples by Uebbing et al.[43] Two Nd:YAG lasers (both operated at 1.06 μm) were used. The first laser (output 13 mJ per pulse) was focused on the sample surface perpendicularly to vaporize the sample. The beam of the second laser (output 77 mJ per pulse) was directed parallel to the sample surface and 1.5 mm above the surface. It was focused 2 mm behind the middle of the first plasma. The samples were placed in a sample chamber filled with argon. There was a time delay between two laser shots. The detection system was a gatable optical multichannel analyzer. The intensity of the Zn line at 468.014 nm was observed to be more than 10 times stronger than the intensity with the vaporizing laser only.

Cremers and Radziemski carried out an experiment using the long-spark technique for direct detection of beryllium on the filter.[44] A long spark was generated by focusing the beam of a pulsed and Q-switched Nd:YAG laser on the surface with a cylindrical lens of 75 mm focal length. Laser energy of 125 mJ per pulse was used to ensure spark stability. The footprint of the spark on the surface was about 0.1 mm wide and 4–8 mm long, depending on the angle of incidence of the laser beam on the filter. The emission from the induced plasma was collected by another lens in the perpendicular direction and analyzed by a monochromator tuned to the wavelength of 313.042/313.107 nm which is the doublet of $Be^+$. The spectrally resolved light was detected by a PMT. The signal was time-resolved and averaged with a boxcar average.

Mason and Goldberg produced a laser spark in a pulsed magnetic field to characterize the effects of a magnetic field on plasma atomization, excitation, and ionization.[45–47] Both emission and absorption spectroscopy were performed. An eight-turn coil was wound on a 1 inch outside diameter polycarbonate tube and a high-voltage capacitive discharge source was used to generate the pulsed magnetic field. A pulsed hollow cathode lamp was used for the absorbance measurement. The hollow cathode lamp was triggered before the formation of the laser plasma and kept active for over 300 μs in order to output a stable emission. The light was collimated by a lens and, after passing through the coil,

was focused by another lens onto the entrance slit of the monochromator. The emission characteristics were found to have significant radial compression and axial expansion of the laser induced plasma.

In 1987 Cremers used a fused silica incoherent fiber bundle instead of a lens to collect the emission from the laser spark.[48] The cable was 1 m in length and 3 mm in diameter. One end of the cable was positioned next to the focusing lens (50 cm focal length) and the other end of the cable was positioned up against the entrance slit of a spectrograph. When the fiber optic cable was positioned 55 cm from the spark, the light collected by the fiber optic bundle was equivalent to that collected by a lens with an $f$ number of 183. Because of the large acceptance angle of fiber optics, light from a wide angle range will be collected by the fiber and is not changed significantly at the output end. This fiber collection technique is suitable for field measurements because it is insensitive to the spark position changes. Schechter and Valery Bulatov have developed a fine technique using an optical fiber.[49] A multiple optic fiber system, with each fiber pointing at a different region of the spark, was used in their measurement. The light from a different fiber was fed into a computerized imaging spectrometer which was attached to an ICCD detector. The fluctuation in the spark was compensated for by observing different elements at a different region in the spark.

LIBS is a useful technique for in situ field measurements. However, most experimental methods introduced previously are laboratory systems and may not be well suited to field measurements. A field system usually requires minimal optical access to the test facility and minimal on-site alignment. In 1994, researchers from Sandia National Laboratory completed a field demonstration of their prototype system to monitor metals emissions at Clemson University's Vitrification Facility.[50] The main feature of the system was a mirror with a hole at the center to allow the laser beam to pass and to reflect the emission signal from the laser spark (Figure 5). The frequency-doubled Q-switched Nd:YAG laser beam (532 nm) was expanded and collimated to pass through the hole in the mirror. The beam was focused in the effluent stream and produced the spark. The same lens was also used to collect and collimate emission from the spark. The lens was mounted at the end of a probe inserted into the test facility through an optical port. The collected light was reflected by the mirror to turn 90° and forward to other optics coupled to the fiber optic bundle. The fiber optic bundle was connected to the spectrometer and detector. This configuration allowed excitation and detection to be performed collinearly and, therefore, only one optical port was used for access and measurement.

Another approach to backwards LIBS detection was developed at the Diagnostic Instrumentation and Analysis Laboratory of Mississippi State University (Figure 6).[51] The frequency-doubled Q-switched Nd–YAG laser beam was reflected at a harmonic separator to remove its fundamental beam. The 532 nm beam was then reflected to the probe lens through a dichroic mirror that reflects 532 nm and transmits other wavelengths. The beam was focused in the off-gas stream to produce the breakdown. The same lens was also used to collect and collimate emission from the plasma. The LIBS signal was transmitted through the dichroic mirror and coupled to the fiber optic bundle with lenses. The fiber optic bundle was connected to the spectrometer and detector.

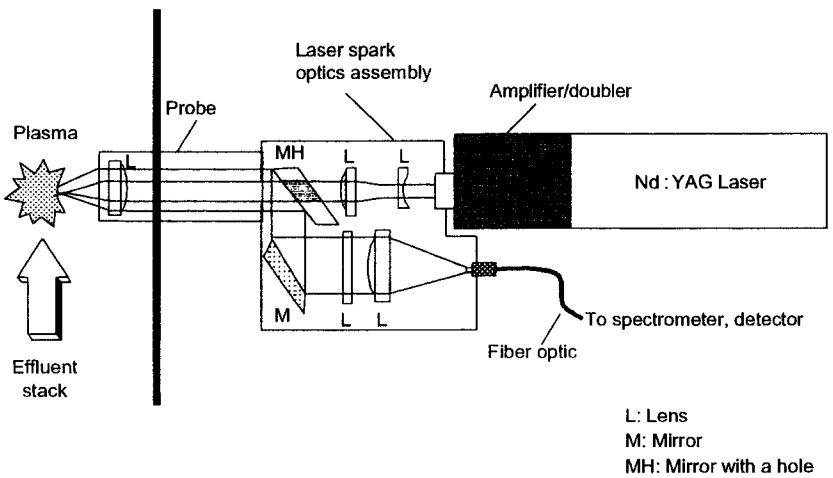


**Figure 5** Diagram of a LIBS system using a mirror with a hole for backward detection. (Reproduced from L.W. Peng et al. *Process Control and Quality*, **7**, 39–49 (1995), by permission of VHC International Science Publishers.)

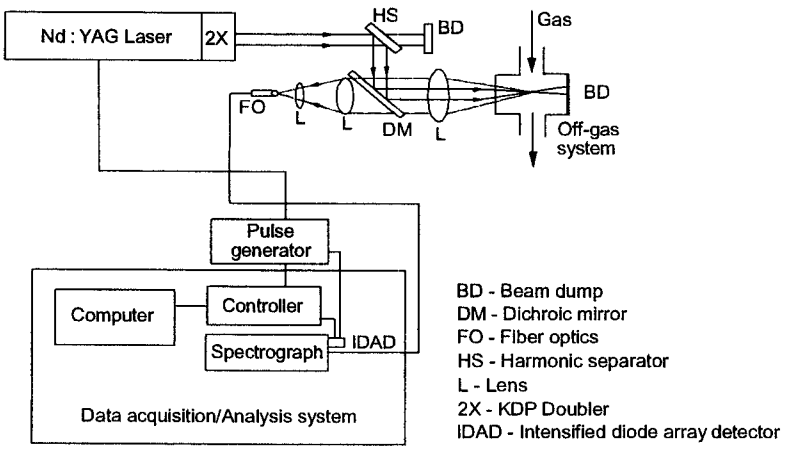


**Figure 6** Diagram of a LIBS system using a dichroic mirror for backward detection.

The rectangular output of the fiber bundle worked as an entrance slit for the spectrometer. This optical configuration, which requires only one port, also allows collinear excitation and detection. It is suitable for real-time measurement in off-gases.

Due to the low breakdown threshold of the optical fiber, optical fibers in early LIBS work were limited to delivering the emission to the detection system. It is now possible to use optical fibers to deliver the laser beam in LIBS applications. Marquardt et al. have recently developed a microprobe for LIBS and Raman measurements using an imaging optical fiber.[52] The microprobe has five separate optical fibers. One 1 mm core diameter silica–silica-clad multimode fiber was used to deliver the Q-switched Nd : YAG laser beam (1.064 μm) for LIBS excitation. A 12 mm focal length lens near the fiber collimated the exited laser beam and a 6.4 mm focal length lens focused the laser beam on the sample. These two lenses were also used to collect spark light and couple the light to another 1 mm core diameter hard-clad fiber which coupled to the spectrograph at another end. The Nd : YAG laser beam delivery fiber was also used to deliver a He–Ne beam to indicate the region of interest on the sample. One image-guide fiber was coupled to a video camera to provide video monitoring while the probe was positioned and aligned for analyzing specific sites on the sample (granite). An ICCD detector was used and operated in gated mode.

### 3.2 Calibration Methods

For practical applications, the measured emission intensities need to be related to the relative or absolute elemental concentration. The system response must be calibrated for a certain measurement. Calibration is the most difficult issue in the development of LIBS, especially for field measurements. LIBS is an atomic emission spectroscopy. In addition to variables related to emission spectra, several other variables greatly affect the intensity of the LIBS signal: the fluctuation of incident laser energy; the size and density of particles and associated matrix effects in the gas flow; the location of the focus point for solid and liquid samples; and the surface feature and the history of ablation by laser shots for solid samples. For on-site measurement, LIBS is considered as a nonsampling technique. However, this implies an extra difficulty for calibration.

For solid sampling, a standard sample can usually be pressed from well-mixed powders. Ernst et al. determined the copper concentration in steel using LIBS.[53] They prepared cylindrical calibration samples using a hot isostatic press process. The flat surfaces of the sample were polished with a soft polishing wheel and cleaned. Eleven samples containing from 0.01% to 5.00% copper were used to obtain a quadratic calibration curve. To reduce the effect of some variables, the intensity ratio of Cu/Fe was used, instead of Cu intensity, to infer the calibration curve against the Cu concentration. For some solid samples, instead of pressing, well-mixed powders can be placed in a furnace to be melted and then frozen.

For gas-phase sampling, a nebulizer is widely used to produce a dry aerosol from a solution of standard reference materials. During a United States Environmental Protection Agency (USEPA) metal CEM test in 1996, a pneumatic nebulizer was used to produce an aerosol flow containing certain concentrations of metal.[54] The nebulizer was enclosed in a separate cell and was inserted into the optical path when the calibration was required.

During the same CEM test, an on-site calibration was performed at the Rotary Kiln Incinerator Simulator.[55,56] An ultrasonic nebulizer (USN) was used to generate a dry metal aerosol from the standard solution which was pumped into the USN with a peristaltic pump. The aerosol was brought to the gas stream through a sample injection probe. The probe tube was mounted on the opposing port against the optical probe across the gas stream. The laser beam was focused 2 cm above the end of the injection probe.

In some cases, if the absolute concentration calibration is too difficult to obtain, the relative concentration may be considered. According to Equation (2), relative concentration can be inferred by fit or by intensity comparisons of two or more different elements in one LIBS spectrum.[57] In addition to the spectroscopic constants, the plasma temperature and degree of ionization are required to perform this calculation. However, these two parameters are not easily determined accurately. An alternative approach to obtaining the relative concentration was the use of reference line intensity information from the National Institute of Standards and Technology (NIST) collections to perform spectral fitting.[58] However, the excitation condition need to be checked for this simple method because the intensities in these reference collections are obtained under conditions which differ considerably from induced plasma.

The techniques for LIBS calibration, especially for field calibration, lags behind the development of LIBS itself. Scientists are still working to solve this problem.

## 4 ENVIRONMENTAL APPLICATIONS

LIBS has the capability to perform rapid, on-site analysis in harsh environments. It can significantly reduce the time and costs associated with sample preparation required by convention analytical techniques and is therefore a promising technique for environmental monitoring and process control.[59] LIBS has been applied to many environmental situations. The major interests here are applications in environmental monitoring and in industrial process control. Other application areas, e.g. clinical, metals, etc., are discussed elsewhere.[60]

### 4.1 Off-gas Emission

The detection of trace metals in the off-gas from waste processing is very important for public health. Conventional analytical techniques require sending a sample to a laboratory for analysis. LIBS can perform in situ off-gas measurement by focusing the laser beam on the gas stream through a window and collecting the signal through an optical fiber. Radziemski and Cremers applied LIBS to the analysis of effluent gases from a prototype fixed-bed coal-gasifier at the Department of Energy Morgantown Energy Technology Center.[31] They demonstrated that LIBS had the capability for near real-time monitoring of the concentrations of major and minor species in the off-gas emission. Neuhauser et al. tested their on-line Pb aerosol detection system with aerosol diameters between 10 and 800 nm. A detection limit of 155 $\mu g\,m^{-3}$ was found.[61] Singh et al. have demonstrated LIBS as a process monitor and control tool for waste remediation.[62] They monitored the toxic metals from three plasma-torch test facilities and proved that LIBS can be integrated with a torch-control system to minimize toxic metal emission during plasma-torch waste remediation.

To use LIBS as a CEM requires the quantitative trace-level determination of toxic metals. The challenges here are to overcome the problems of this technique related to poor detection sensitivity for some elements, limited accuracy and precision, and difficulty of calibration for in situ analysis. With a sensitive ICCD detector and properly selected experimental set-up, the sensitivity and precision has been greatly improved. However, on-line calibration is still a big problem for CEM-type applications due to difficulties of introducing known amount samples into the off-gas system.

Singh et al. investigated the possibility of using metal hydrides to calibrate metals in off-gas emissions.[63] They used a static sample cell to perform LIBS experiments on metal hydrides and found the LIBS signal to be affected by gas composition, gas pressure, and laser intensity. They also found that the LIBS signal intensity for metal hydrides changes with time. The time at which the signal reaches its peak also depends on the concentration of the sample. Therefore the selection of different time periods for the LIBS measurement will be critical for LIBS calibration. They suggested that a flowing metal hydride sample cell system might solve some of the problems related to the static system they used.

Detection of Hg in off-gas emission has been reported by several researchers. Lazzari et al. performed LIBS to detect Hg in air in a laboratory.[64] The Hg vapor was successively diluted in a chamber, and a Nd:glass laser (1064 nm, 180 mJ) was used to produce plasma in the Hg vapor. They reported a very low detection limit of 42 $\mu g\,m^{-3}$ for Hg using the Hg 253.7 line. Singh et al. used an USN to generate a known concentration of metal aerosol in a sample cell and found the minimum detectable Hg level to be approximately one order higher than that reported by Lazzari et al.[64] The reported Hg detection limit with a pneumatic nebulizer is consistent with the result with an USN.[65] The reason for a higher Hg detection limit with a nebulizer system is unclear. One possible explanation is that the aerosol-induced

breakdown might cause incomplete atomization of larger particles in the colder region of the plasma and this results in a higher Hg detection limit.

The laboratory-tested calibration technique is successful for simulated effluent in a sample cell using an aerosol generator. However, it cannot be directly applied to samples from the practical environment due to difficulties in reproducing the plasma conditions under quite different sampling conditions (i.e. particle size, gas flow, temperature, pressure, etc.). As a result of the difficulties in injecting a known amount of sample into a gas stream, researchers are now exploring the possibility of using an internal reference for self-calibration. The internal reference has to be a major species in the gas medium. The concentrations of the internal reference must be known to an accuracy below 10%. This calibration method is intended for compensating plasma condition changes due to the variation of gas stream conditions or laser pulse-to-pulse fluctuations. Therefore, the plasma temperature has to be inferred from the reference lines. The intensity ratio of the analyte line and the reference line are corrected based on the inferred plasma temperature. Loge has tested this calibration procedure for LIBS CEM using $N_2^+$ lines to determine plasma temperature and to monitor the changes in the plasma condition.[66] The observed emission line intensities were adjusted based on the inferred plasma temperature, and the concentration was extracted from the plasma temperature-corrected calibration curve. However, the plasma condition is not only characterized by plasma temperature. Electron density can also affect the degree of ionization of the probed atoms and hence the signal of the neutral or ion line. Furthermore, this calibration relys on the plasma temperature extracted from the intensity ratio of two emission lines, which is known to be an inaccurate method for plasma-temperature determination. This calibration might be suitable for LTE conditions in which and electron density and plasma temperature are not significantly different from the calibration condition. However, the success of this internal calibration method will greatly depend on the plasma characteristics and matrix effect.

LIBS has low sensitivity for some elements in off-gas measurements because of its small sample volume. Hahn et al. developed a technique based on random sampling and conditional analysis to solve the problem associated with finite sample volume and size distribution of the target metal.[67] They compared Monte Carlo simulation with the experimental results and claimed considerable enhancement with this technique for low metal concentrations where only a few single-shot spectra contained the desired metal emission. This calibration technique seems promising; however, more tests are required to prove its validity for different sampling conditions.

LIBS has been tested as a multimetal CEM. Using concentrations as specified by the Resource Conservation and Recovery Act (RCRA), metals were measured and the results compared with the USEPA's reference method.[65] A relative precision of 50% and a relative accuracy (RA) of 78% or better were obtained from these tests. The rapid sampling rate and potential for metal CEM are demonstrated in this test. However, the sensitivity and accuracy for certain toxic metals will need to be further improved before LIBS can be accepted as a metal CEM by the USEPA.

### 4.2 Metal and Glass

Kurniawan et al. have applied LIBS to the elemental analysis of glass.[68] They found the detection limits are much lower than those usually required for glass with low surrounding pressure (1–5 torr). In addition, light elements (such as Li and B) that are usually difficult to observe by X-ray fluorescence were also successfully detected with a detection limit less than 10 ppm. Thiem et al. performed LIBS measurements on alloys in an ultrahigh vacuum ($<5 \times 10^{-7}$ torr).[69] They found the background signal is significantly reduced in comparison to that from an atmospheric environment. This makes a simultaneous, multielement analysis in very complex solid samples possible. They obtained calibrations for Al, Fe, Cu, Ni, and Zn using a standard reference material and found the detection limit to be matrix dependent. Absolute detection limits were estimated to be in the 20–200 $\mu g\, g^{-1}$ range for the above elements. Sabsabi and Cielo made quantitative analyses of aluminum alloys with LIBS.[70] To find the optimum condition for LIBS analysis, they first studied laser plasma characterization by extracting plasma temperature and electron density with Fe and $Al^+$ lines, respectively. They found plasma temperatures are close to a constant within experimental uncertainty at 10 μs delay and 10 μs gate width with different concentrations of Mg in aluminum alloys. Calibration curves for Mg, Mn, Cu, and Si were constructed under this optimum experimental condition. The Mg calibration based on the 285.2 nm resonance line shows problems of self-absorption at higher concentrations, whereas the calibration based on nonresonance 518.36 nm and 517.27 nm Mg lines is linear for the same concentration range. The precision and detection limits for LIBS analysis of aluminum alloy were calculated based on the calibration data. They found a relative standard deviation (RSD) of better than 6% and detection limits better than 15 ppm for all the elements studied.

The current process for molten steel analysis includes collecting a molten sample, cooling it, and then transporting it to a nearby analytical laboratory for analysis. It is a time- and labor-intensive process. The hot melt composition might change due to vaporization of the more

volatile components during this period. Also, compositional fluctuations cannot be effectively monitored with the current analysis method. LIBS has the capability of performing on-line measurements, which can reduce the data processing time and reduce the cost for the steel industry.

Argagon et al. have demonstrated the application of LIBS to molten steel.[71] To measure the carbon content they used an argon atmosphere to reduce carbon emission from dissociated CO or $CO_2$. As the composition of the molten surface may not represent the bulk melt, an Ar jet was applied on the surface of molten steel to measure the bulk concentration during the measurement. A C/Fe detection limit of 250 ppm with a RSD of 6% was found. Lorenzen et al. developed an on-line monitor for molten steel.[59] Elemental concentrations were determined based on calibration of the intensity ratio of an analyte line and a reference line versus elemental concentration. To ensure measurement accuracy, they also monitored the plasma condition using the intensity ratio of an atomic/ionic line pair. When a change in the plasma condition was detected, a proper correction factor was applied to the calibration curve. Paksy et al. also performed LIBS on the surface of a molten alloy using an Nd:YAG laser.[72] They compared the measurement with argon and air atmospheres and found that the Ar atmosphere prevents surface oxidation and gave a higher *S/B* with good precision for a relative intensity measurement. Detection limits for Si/Fe, Mn/Fe, Cr/Fe, Si/Al, and Mn/Al were found to be 10 ppm, 50 ppm, 40 ppm, 600 ppm, and 70 ppm respectively.

The application of LIBS to solid/molten materials is very promising. However, problems such as matrix effects (selective vaporization), sensitivity for all the element of interest, calibration, precision, and accuracy still need to be solved for quantitative measurement. Although it cannot provide the high accuracy and precision of laboratory-based methods, it has great potential as a process control monitor in the steel and glass industries by providing rapid, semiquantitative composition measurements in a remote location.

### 4.3 Soil, Concrete, and Paint

The detection of contaminated soil and concrete is another challenging area for LIBS. Yamamoto et al.[73] have used a portable LIBS system to detect toxic metals in soil, finding Ba, Be, Pb, and Sr in soil with detection limits of 265, 9.3, 298, and 42 ppm, respectively. Cremers et al. have detected Ba and Cr in soil using an optical fiber probe.[74] Limits of detection (LODs) of 26 ppm and 50 ppm were found for Ba and Cr, respectively. Eppler et al. have studied the matrix effect in soil. They found LODs for Pb and Ba in a sand matrix were 17 and 76 ppm (by weight), respectively, with a precision of 7% RSD or less.[75] In soil, the detection limits were 112 and 63 ppm (w/w) for Pb and Ba, respectively, with 10% RSD precision. The LIBS signal was affected by chemical speciation as well as matrix composition. LIBS accuracy can be degraded if calibrations are not compound and matrix specific. The accuracy of LIBS measurement in soil is affected by many factors. It is presently more suitable as an initial screening of highly contaminated soils to determine the remediation boundary of the contaminated area.

LIBS for detection of lead in contaminated concrete was explored by Pakhomov et al.[76] They used a Q-switched Nd:YAG laser (10 Hz) to perform time-resolved LIBS for quantitative measurement of the lead content in concrete. Pb calibrations were obtained for different delay times using the ratio of the integrated emission line of lead (405.78 nm) to an oxygen line (407.59 nm). They found the absolute Pb signal is independent of the laser pulse energy for laser energies between 250 and 400 mJ. Based on analysis of the sensitivity of lead measurements at different delay times, they derived a best Pb detection limit of 10 ppm in concrete at an optimum delay time of 3.0 μs.

Lead in paint is known to be a potential health threat, especially to children. The feasibility of using LIBS to determine Pb in the paint surface has been successfully demonstrated by Yamamoto et al. using a portable LIBS system.[73] The temporally integrated LIBS signal is recorded with an nongateable charge-coupled device (CCD) detector. Because of the problem of spectral interference associated with the Pb 405.73 nm line, they used a weaker $Pb^+$ line at 220.35 nm for calibration. They obtained a Pb detection limit of 0.8% (8000 ppm) in paint with an RSD between 23% and 47%. Marquardt et al. used a fiber optics LIBS system to determine Pb in paint.[52] They used a gate delay of 3.0 μs and gate width of 12.6 μs in the measurements. They reported a LOD of 140 ppm for Pb with a precision of 5–10% using the Pb 405.78 nm line.

### 4.4 Air Sampling Filters

Direct detection of trace element in air with LIBS is very difficult due to its insufficient sensitivity. For trace metals below the LIBS detection limits, an air sample can be collected on a filter which is then subsequently analyzed by LIBS. This method has a lower detection limit and provides a quasi-on-line measurement. Arnold and Cremers have used this technique to determine metal particles on an air damping filter.[77] They used a cylindrical lens to form a long spark on the filter to increase the sample volume and reduce the filter damage. Using the calibration curve for Tl line at 535.05 nm, a LOD of 40 ng $cm^{-2}$ for Tl in filter paper was obtained. Later, Yamamoto et al.

determined LODs of 21 ng $cm^{-2}$ and 5.6 μg $cm^{-2}$ for Be and Pb on a filter.[73] They also noticed that particle size can affect the detection limit for filter analysis. Cremers and Radziemski have measured Be on a filter surface and found that Be particles greater than 10 μm on the filter were not completely vaporized. The particle size dependence of the LIBS signal puts a restriction on LIBS application to air sampling through a filter.[44]

### 4.5 Radioactive Materials

LIBS has been used to monitor the level of radioactive elements in a process stream. Wachter and Cremers found a detection limit of 100 ppm for uranium in solution.[34] To overcome poor shot-to-shot precision due to small variations in the lens-to-sample distance, they had to average 1600 laser shots for analysis. To investigate the feasibility of applying LIBS to detect radioactive elements, Singh et al. recorded LIBS spectra of U, Pu, and Np in a glove box.[78] Emission lines suitable for detection of these radioactive elements were identified. Their preliminary study showed that LIBS is suitable for the measurement of radioactive elements in waste streams. Ernst et al. used LIBS as a tool for detection of radiation embrittlement in a nuclear power plant by determining the Cu concentration in A533b steel.[79] As Cu is the key impurity contributing to radiation embrittlement, the Cu concentration in the steel is an indicator of radiation embrittlement and of expected material lifetime. Due to the hazardous environment, a fiber optic delivery system was initially used in the measurement. However, the optical fiber system could not deliver sufficient laser energy for sensitive Cu detection. Copper concentrations between 100 ppm and 5% were later detected using a conventional all-optic beam delivery system. Their measurements demonstrated that LIBS can provide quick, accurate, and remote detection for monitoring the reactor pressure vessel material.

## 5 COMPARISON WITH OTHER SPECTROSCOPY TECHNIQUES

The LIBS technique has several advantages compared to conventional emission methods. In LIBS, a high-energy pulsed laser beam is used to produce atomic emissions from the focal volume. Hence it provides time and spatially resolved measurement. It requires only a small amount of sample and minimal sample preparation. Gated detection with an intensified detection system discriminates the background emission and also improves the detection limit. With properly selected atomic lines, multiple species can be simultaneously monitored in a spectral region. Furthermore, as a laser spark can be generated in a remote location, it has remote monitoring capability. In this section the accuracy of LIBS is compared with some spectroscopic techniques commonly used in the laboratory, such as AAS, ICPAES, and XFS.

AAS is used to detect the presence and amount of metal atoms in very dilute solutions. It is widely used in laboratories that analyze the purity of water. The resonant wavelength of choice from a selected spectral lamp passes through the sample vapor. The atomized element absorbs the light energy over time. The concentration is determined through a calibration curve. The sample solution can be atomized by passing an electrical current through a graphite tube which contains the analyte (graphite furnace atomic absorption (AA)) or using a flame to atomize the sample (flame AA). The graphite furnace AA technique often offers about 1000-fold sensitivity improvement as compared with flame AA.

ICPAES measures the intensities of light emitted from each species as they are atomized and perhaps ionized in the plasma. As an AES (atomic emission spectrometry) technique, ICPAES has the capability of simultaneous multielement measurement. Atomization is more complete in the ICP (inductively coupled plasma) system than in the AAS system; therefore, LOD values are generally lower for ICPAES than for AAS. However, because the temperature of ICP is much greater than for AAS, spectral interference tends to be a greater problem for ICPAES than for AAS. The temperature cross-section of the plasma is relatively uniform; as a consequence, self-absorption and self-reversal effects are not encountered.

XFS is a spectroscopic method that is commonly used for solids in which secondary X-ray emission is generated by excitation of a sample with X-rays. The X-rays eject inner-shell electrons. Outer-shell electrons take their place and emit photons in the process. The photon wavelength depends on the energy difference between the outer-shell and inner-shell electron orbitals. The amount of fluorescence is very sample dependent and quantitative analysis requires calibration with standards with a similar matrix. XFS can provide rapid quantitative analysis for various samples. However, XFS is not applicable to light elements ($M < 10$) such as Be, B, and Li. As the XFS signal is generated from a significant thickness of sample within which absorption and scattering can occur. It is known to suffer significant disturbance from the matrix which is caused by either absorption from the matrix elements or enhancement by the emission of a matrix element.

### 5.1 Sample Preparation

Laser plasma is a direct sampling and excitation tool. Only small amounts of samples are used. The laser prepares

and excites the sample in one step. Therefore, minimal sample preparation is required compared to conventional techniques. It also avoids possible contamination by tedious and time-consuming sample preparation procedures. However, because a minimal amount of sample is ablated and analyzed, the precision and accuracy of measurements depends on the homogeneity of the sample.

Typical sample preparation in AAS involves dissolving a solid sample in an acidified solution. Aqueous dilution with the appropriate acid, ionization suppression agent(s), or matrix modifier(s) may be necessary. The diluted solution is aspirated into an atomizer (i.e. flame or furnace) to atomize the sample. Air samples are collected with a filter. The particles collected on the filter are dissolved in acid to produce a solution which is analyzed with conventional AA. Flame AA utilizes milliliters of sample. Graphite AA typically uses about 20 μL of sample. The sample preparation procedure for AAS is generally time-consuming which is not conducive to online and in situ measurement.

In ICPAES, the sample may be an aerosol, a thermally generated vapor, or a fine powder. The sample is carried into the hot plasma at the head of the tubes by argon flowing at about 1 L $min^{-1}$ through the central quartz tube of the ICP torch. Typically, the sample is reduced to a solution that is nebulized into the ICP system. An autosampler is frequently used to supply solutions (including blanks, standards, and sample) to the plasma sequentially. It is an attractive technique for the analysis of geological material due to its multielement capability. However, samples need to be dissolved prior to analysis. Various chemical schemes are necessary to dissolve as many elements into solution as possible. Thiem and Wolf have compared the analysis of Al ores from the NIST by ICPAES and LIBS.[80] In ICP measurements, the powder samples are first dried in an oven at 140 °C for 2 h. A specific weight of dried sample is then digested with a mixture of concentrated HCl and deionized water in a digestion flask at 90 °C overnight. The digested samples are then put into a volumetric flask for analysis. When using LIBS to analyze the same type of sample, a small amount of sample was compressed into a disk. The sample attached to a sample translation device is then placed into the sampling chamber. The LIBS measurement started after the sampling chamber was evacuated to about 1 mtorr. The required sample preparation time (including time required to pump down the sampling chamber) for LIBS analysis is less than one hour which is much shorter than that required for an ICP measurement.[80]

XFS can be used to analyze a variety of samples. Liquid samples, from water to oil, require essentially no preparation. Many solid samples, if homogeneous, can be machined to the proper shape and run directly. Inhomogeneous samples, such as ores and biological materials, must be pulverized or fused. Then the homogenized material can be dissolved for analysis as a liquid sample, pressed into pellet form, or cast as a glass-like solid. XFS can also be used for the analysis of atmosphere pollutants. The air sample is first collected through a stack consisting of micropore filters and is then analyzed by XFS directly. Although XFS has direct sampling capability, it suffers more severe matrix effects with direct sampling than does LIBS. Also, XFS does not have remote analysis capability, whereas LIBS can use optical fibers to perform remote measurements.

Comparing LIBS with ICP, AAS, and XFS, LIBS and XFS require minimum sample preparation. AA and ICP require destructive and relatively tedious and time-consuming pretreatment of the samples, which is likely to introduce uncontrollable error in the measurements.

### 5.2 Sampling Rate

LIBS is an optical emission based-technique. It can perform multielement measurements. Generally LIBS can produce useful results in 3–60 s. The sampling rate depends on the laser repetition rate and sample concentration. XFS spectra are relatively simple and the technique is nondestructive. The speed (1–10 min) and convenience of the procedure permits multielement analyses to be completed in a few minutes ICP and AAS can have a sampling time of less than 1 min. However, sample preparation often takes several hours. It takes minutes to hours for complete sample analysis.

### 5.3 Detection Limit

The detection limit is the minimum concentration that can in principle be measured. It is generally defined as the concentration that produces a signal three times larger than the SD of the background. As multielement techniques, LIBS, ICPAES, and XFS all rely on being able to resolve spectral signals unique to each element. When the signals of some elements are very strong, they start to interfere with weaker signals from the other elements, and it may be difficult to achieve the optimum detection limits. LIBS has poorer sensitivity in gas measurements due to the low concentration and small laser microplasma. Typical LODs for LIBS are in the ppm to percentage range. For ICPAES, detection limits for most elements are of the order of 10 ppb.

XFS is generally less sensitive than the various optical methods. It offers LODs from a few ppm to the percentage range. In AAS, the amount of light that is absorbed by the sample is directly proportional to the concentration of the ground state element of interest in that aspirated sample. Some samples may have matrix, chemical, and/or ionization interferences. When recognized, each interference can usually be controlled to yield meaningful

sample analysis. Detection limits ranging from around $3 \times 10^{-4}$ ppm to 20 ppm are observed for various metallic elements using flame AA. Graphite furnace atomic absorption spectrometry (GFAAS) often reduces this limit by a factor of 10–1000.

This direct comparison of LIBS detection limits with other analytical techniques is unrealistic because of the different samples used. In general, LIBS still cannot match the detection limits of most conventional analytical techniques in most cases. However, its ability to directly analyze samples without cumbersome sample preparation has led to its promising application in practical field determinations of elements for environment and industrial samples.

### 5.4 Accuracy and Precision

Precision and accuracy are generally used to determine the merit of a measurement technique. Precision is the measure of the degree of reproducibility of a measurement. It is generally measured as the RSD of a set of repeated measurements. Accuracy is used to determine the difference between the evaluated measurement method and a measurement by a standard method. It is generally expressed as the RA. The size and excitation characteristics of a LIP can affect the amount of sample vaporized and the degree of excitation, and hence affect the LIBS accuracy and precision. Typical LIBS precision is 5–20%. Laser shot-to-shot variation causes differences in the plasma properties and therefore affects the magnitude of the element signal and hence degrades the LIBS precision. To improve LIBS precision, spectra from several laser shots have to be averaged in order to reduce statistical error due to laser shot-to-shot fluctuation.

The accuracy of LIBS depends on the sample composition, homogeneity, surface condition, and particle size generated. The sample matrix can affect the amount of element ablated and hence the LIBS signal. As LIBS only analyzes a small amount of sample, the result might be biased if the composition of the ablated sample does not represent the composition of the bulk. Multipoints measurements can improve the LIBS accuracy for an inhomogeneous sample.

For LIBS measurements based on the theoretical analysis of emission line intensity ratios, the accuracy depends greatly on the available spectroscopic constants, inferred temperature, and electron density. The uncertainty in these parameters is generally larger than 25%. Therefore, this is not a very accurate analysis method for LIBS. The best estimated accuracy with this technique is about 10%.

If the LIP condition is reproducible, calibration by emission line intensity is a more promising analysis tool for LIBS. The accuracy of this technique relies on absolute intensity measurement and therefore is affected by laser shot-to-shot fluctuation and particle size. Also this type of calibration shows a loss of sensitivity at high analyte concentrations due to self-absorption in the laser plume.

The sensitivity of AAS is dependent on the element, but is usually in the ppm region for flame AA and ppb region for graphite AA. Sample concentration techniques enable detection at even lower levels. Its precision is a function of several preparative, elemental, and instrumental conditions. Typically, the RSD associated with a flame absorption analysis is of the order of 1–2%. With caution, this figure can be lowered to a few 10ths of 1%.

The measurement precision of ICPAES is typically 1–5%. Thiem and Wolf have analyzed mining ores with both LIBS and ICPAES.[80] The elements Al, Ca, Cu, Fe, K, Mg, Mn, Si, and Ti were determined in aluminum and manganese ore. In these measurements, LIBS obtained an RA of 0.5–20% and ICP an RA of 0.7–14%. Overall results show that ICP has better precision than LIBS (Table 2).

The potential of LIBS as a screening instrument in field work was recently evaluated, based on its accuracy and precision. Yamamoto et al. have compared the performance of a portable LIBS with a commercial portable XFS unit.[73] They used certified reference soil as the test sample to determine Sr concentration in soils. XFS measurements were obtained from a Spectrace™ 9000 portable XFS unit with 200 s integration time and LIBS was performed with 10 s integration time (10 laser sparks). The certified soils have Sr concentrations in the range 26–380 ppm. The test results are shown in Table 3. Sr concentrations were measured from all the samples with LIBS except the sample containing 26 ppm Sr, which is below its detection limit. The LIBS precision was found to be in the range 3–18% and the XFS precision was between 3% and 23%. The RA obtained from these measurements were 0–44% for LIBS and 9–44% for XFS. The portable LIBS therefore has comparable accuracy and precision to a portable XFS unit. However, the portable LIBS has slightly poorer sensitivity for Sr than the portable XFS unit. This study indicates that LIBS has the same capability as an in situ screening device for soil as XFS.

**Table 2** Comparison of LIBS and ICP measurement of NIST Al ore samples[80]

| Element | NIST certified value | ICP | LIBS |
|---|---|---|---|
| Al | 25.52 ± 0.40 | 25.34 ± 0.39 | 24.3 ± 1.2 |
| Ca | 0.443 ± 0.020 | 0.404 ± 0.02 | 0.427 ± 0.010 |
| Fe | 13.71 ± 0.20 | 13.44 ± 0.1 | 13.63 ± 0.75 |
| Mg | 0.035 ± 0.008 | 0.038 ± 0.01 | 0.028 ± 0.008 |
| Mn | 0.294 ± 0.030 | 0.252 ± 0.01 | 0.25 ± 0.05 |
| Si | 0.323 ± 0.03 | 0.305 ± 0.05 | 0.275 ± 0.03 |
| Ti | 1.43 ± 0.07 | 1.52 ± 0.10 | 1.32 ± 0.15 |

**Table 3** Comparisons of determination of Sr in soil using LIBS and the ICP.[73]

| Certified soil | Actual concentration (ppm) | LIBS (ppm) | LIBS %RSD | XFS (ppm) | XFS %RDS |
|---|---|---|---|---|---|
| 07401 | 155 | 87 | 5.3 | 200 | 5.9 |
| 07402 | 187 | 187 | 5.1 | 221 | 4.9 |
| 07403 | 380 | 295 | 4 | 434 | 3.2 |
| 07405 | 42 | 30 | 17.5 | 48 | 13.6 |
| 07406 | 39 | 28 | 12 | 56 | 14.4 |
| 07407 | 26 | [a] | [a] | 35 | 22.9 |
| 07408 | 236 | 204 | 3.2 | 257 | 4.5 |

[a] Sr signal was not detectable.

As a result of the small sample volume used the analytical capabilities of LIBS are generally poorer than most conventional methods. However, various studies have shown that LIBS is best for applications where standard laboratory instrumentation is not feasible, such as measurements in remote or harsh environments.

## 6 FUTURE DEVELOPMENTS

The development of LIBS has progressed rapidly since that late 1980s, with work on improving LIBS measurement of gas, liquid, and solid samples. The following research areas need to be strengthened before the technology reaches maturity for commercialization.

LIBS application as a CEM needs work on improving calibration methods, sensitivity and accuracy. An on-line calibration method needs to be developed for off-gas emission measurements. Sensitivity can be improved either by increasing the signal or reducing the background noise from the plasma and detector. Accuracy of the measurement can be improved by reducing pulse-to-pulse fluctuations of the laser-induced spark. Some toxic metals have analytical lines shorter than 200 nm, whereas optical fiber capability and detector sensitivity decrease considerably in this spectral region. Further work is therefore needed to improve measurement in this spectral region.

Further work is also required for the application of LIBS to the analysis of liquid samples. The main research areas of interest are studies of *S/N* for the laser spark produced with different liquid surfaces and bulk liquids, and techniques to measure concentrations at various depths. Quantitative measurement of solid samples with LIBS needs additional research to improve its analytical capabilities by improving the pulse-to-pulse spark reproducibility and laser ablation. Hybrid techniques such as combining LIBS with other discharge excitation sources need to be further tested to improve LIBS analytical capabilities. Matrix effects on concentration measurements also need further investigation. LIBS has great potential for molten metal/glass applications. However, more detailed studies of LIBS on molten materials are needed.

To develop LIBS as a mature environmental analytical technique, work to commercialize a field LIBS instrumentation is also needed. Instrument size and cost should be reduced. A spectrometer that can measure simultaneously all the elements of interest needs to be developed.

## ACKNOWLEDGMENTS

The authors are thankful to Dr D.L. Monts and Ms L. Wade for a critical review of the manuscript. This work was supported by DOE contract DE-FG02-93CH-10575.

## ABBREVIATIONS AND ACRONYMS

| | |
|---|---|
| AA | Atomic Absorption |
| AAS | Atomic Absorption Spectrometry |
| AES | Atomic Emission Spectrometry |
| CCD | Charge-coupled Device |
| CEM | Continuous Emission Monitor |
| GFAAS | Graphite Furnace Atomic Absorption Spectrometry |
| ICCD | Intensified Charge Coupled Device |
| ICP | Inductively Coupled Plasma |
| ICPAES | Inductively Coupled Plasma Atomic Emission Spectrometry |
| LIBS | Laser-induced Breakdown Spectroscopy |
| LIP | Laser-induced Plasma |
| LOD | Limit of Detection |
| LTE | Local Thermal Equilibrium |
| LTSD | Lens-to-Surface Distance |
| NIST | National Institute of Standards and Technology |
| PMT | Photomultiplier Tube |
| RA | Relative Accuracy |
| RCRA | Resource Conservation and Recovery Act |
| RSD | Relative Standard Deviation |
| RSP | Repetitive Spark Pair |
| RSS | Repetitive Single Spark |
| *S/B* | Signal-to-background Ratio |
| *S/N* | Signal-to-noise Ratio |
| TEA | Transversely Excited Atmospheric Pressure |
| USEPA | United States Environmental Protection Agency |
| USN | Ultrasonic Nebulizer |
| UV | Ultraviolet |
| XFS | X-ray Fluorescence Spectroscopy |

## RELATED ARTICLES

*Coatings* **(Volume 2)**
Atomic Spectroscopy in Coatings Analysis

*Environment: Trace Gas Monitoring* **(Volume 3)**
Automotive Emissions Analysis with Spectroscopic Techniques

*Environment: Water and Waste* **(Volume 3)**
Heavy Metals Analysis in Seawater and Brines

*Environment: Water and Waste* cont'd **(Volume 4)**
Laser Ablation Inductively Coupled Plasma Spectrometry in Environmental Analysis • Optical Emission Inductively Coupled Plasma in Environmental Analysis • Sample Preparation for Environmental Analysis in Solids (Soils, Sediments, and Sludges) • Sampling Considerations for Biomonitoring • X-ray Fluorescence Spectroscopic Analysis of Liquid Environmental Samples

*Field-portable Instrumentation* **(Volume 4)**
Portable Instrumentation: Introduction

*Food* **(Volume 5)**
Sample Preparation for Food Analysis, General

*Atomic Spectroscopy* **(Volume 11)**
Atomic Spectroscopy: Introduction • Laser Ablation in Atomic Spectroscopy • Laser Spectrometric Techniques in Analytical Atomic Spectrometry • Laser-induced Breakdown Spectroscopy • Microwave-induced Plasma Systems in Atomic Spectroscopy

## REFERENCES


1. G. Bekefi (ed.), *Principles of Laser Plasma*, John Wiley & Sons, New York, 1976.
2. L.J. Radziemski, D.A. Cremers (eds.), *Laser Induced Plasma and Application*, Marcel Dekker, New York, 1989.
3. L.J. Radziemski, R.W. Solarz, J.A. Paisner (eds.), *Laser Spectroscopy and Its Applications*, Marcel Dekker, New York and Basel, 1987.
4. R.S. Adrain, J. Watson, 'Laser Microspectral Analysis: A Review of Principles and Application', *J. Phys. D: Appl. Phys.*, **17**, 1915–1940 (1984).
5. V. Majidi, M.R. Joseph, 'Spectroscopic Applications of Laser-induced Plasma', *Crit Rev. Anal. Chem.*, **23**(3), 143–162 (1992).
6. D.C. Smith, R.G. Meyerand, Jr, 'Laser Radiation Induced Gas Breakdown', in *Principles of Laser Plasma*, ed. G. Bekefi, John Wiley & Sons, New York, 457–507, 1976.
7. S.I. Anisimov, V.A. Khokhlov, *Instabilities in Laser-Matter Interaction*, CRC Press, Boca Raton, 1995.
8. R.G. Tomlinson, E.K. Damon, H.T. Buscher, 'The Breakdown of Noble and Atmospheric Gases by Ruby and Neodymium Laser Pulses', in *Physics of Quantum Electronics*, eds. P.L. Kelley, B. Lax, P.E. Tannenwals, McGraw-Hill, New York, 1966.
9. V.N. Pozhidaev, A.I. Fatievskii, 'Optical Breakdown Thresholds in Liquid Water and Micron Size Water Droplets Exposed to Single Laser Pulses', *Sov. J. Quantum Electron.*, **11**, 65–68 (1981).
10. J.F. Roach, J.M. Davies, 'Electric Strength of Some Liquid Dielectrics Subjected to a Q-switched Laser Pulse', *Proc. IEEE*, 1388–1390 (1970).
11. B.G. Gorshkov, Y.K. Danileiko, A.S. Lobachev, V.A. Lobachev, A.A. Manenkov, A.V. Sidorin, 'Laser Induced Breakdown in Alkali Halides', *Sov. Phys. JETP*, **45**, 612–618 (1977).
12. G.M. Weyl, 'Physics of Laser-induced Breakdown: An Updata', in *Laser Induced Plasma & Application*, eds. L.J. Radziemski, D.A. Cremers, Marcel Dekker, New York, 1989.
13. C.A. Bye, A. Scheeline, 'Saha–Boltzmann Statistics for Determination of Electron Temperature and Density in Spark Discharge Using an Echelle/CCD System', *Appl. Spectrosc.*, **47**, 2022–2039 (1993).
14. J.A. Woodroffe, J. Hsia, A. Ballantyne, 'Thermal and Impulse Coupling to an Aluminum Surface by a Pulsed KrF laser', *Appl. Phys. Lett.*, **36**, 14–15 (1980).
15. H.T. Buscher, R.G. Tomlinson, E.K. Damon, 'Frequency Dependence of Optically Induced Gas Breakdown', *Phys. Rev. Lett.*, **15**, 847–849 (1965).
16. R.A. Bingham, P.L. Salter, 'Analysis of Solid Materials by Laser Probe Mass Spectrometry', *Anal. Chem.*, **48**, 1735–1740 (1976).
17. F. Dahmain, 'Ablation Scaling in Laser-produced Plasma with Laser Intensity, Laser Wavelength, and Target Atomic Number', *Phys. Fluids B*, **4**, 1585–1588 (1992).
18. G.H. Canavan, W.A. Proctor, P.E. Nielsen, S.D. Rockwood, '$CO_2$ Laser Air Breakdown Calculation', *IEEE J. Quantum Electron.*, **8**, 564 (1972).
19. Y.P. Raizer, *Laser-induced Discharge Phenomena*, Consultants Bureau, New York, 63–102, 1977.
20. B. Wolff-Rottke, J. Ihlemann, H. Schmidt, A. Scholl, 'Influence of the Laser-spot Diameter on Photo-ablation Rates', *Appl. Phys. A*, **60**, 13–17 (1995).
21. R.A. Multari, L.E. Foster, D.A. Cremers, M.J. Ferris, 'Effect of Sampling Geometry on Elemental Emissions in Laser-induced Breakdown Spectroscopy', *Appl. Spectrosc.*, **50**(12), 1483–1499 (1996).
22. M. Kuzuya, H. Matsumoto, H. Takechi, O. Mikami, 'Effect of Laser Energy and Atmosphere on the Emission Characteristics of Laser-induced Plasma', *Appl. Spectrosc.*, **47**, 1659–1664 (1993).
23. Y.I. Lee, T.L. Thiem, G.-Y. Kim, Y.Y. Teng, J. Sneddon, 'Interaction of a Laser Beam With Metals. Part III: The Effect of a Controlled Atmosphere in Laser-ablated Plasma Emission', *Appl. Spectrosc.*, **46**, 1597–1604 (1992).

24. K. Kagawa, S. Yokoi, 'Application of the $N_2$ Laser to Laser Microprobe Spectrochemical Analysis', *Spectrochim. Acta, B*, **37**, 789–795 (1982).
25. D.C. McDonald, 'Temperature, Electron Densities and Degree of Ionization in a Boosted Glow Discharge Emission Lamp', *Spectrochim. Acta, B*, **37**(9), 747–758 (1982).
26. W. Sdorra, J. Brust, K. Niemax, 'Basic Investigation for Laser Microanalysis IV. The Dependence on the Laser Wavelength in Laser Ablation', *Mikrochim. Acta*, **108**, 1–10 (1992).
27. T. Ishizuka, 'Laser Emission Spectrography of Rare Earth Elements', *Anal. Chem.*, **45**, 538 (1973).
28. Z.W. Hwang, Y.Y. Teng, K.P. Li, J. Sneddon, 'Interaction of a Laser Beam with Metals. Part I: Quantitative Studies of Plasma Emission', *Appl. Spectrosc.*, **45**(3), 435–441 (1991).
29. Y.I. Lee, S.P. Sawan, T.L. Thiem, Y.Y. Teng, J. Sneddon, 'Interaction of a Laser Beam with Metals. Part II: Space-resolved Studies of Laser-ablated Plasma Emission', *Appl. Spectrosc.*, **46**(3), 436–441 (1992).
30. B.C. Castle, K. Talabardon, B.W. Smith, J.D. Winefordner, 'Variable Influencing the Precision of Laser-induced Breakdown Spectroscopy Measurement', *Appl. Spectrosc.*, **52**(5), 649–657 (1998).
31. L.J. Radziemski, D.A. Cremers (eds.), *Laser-induced plasma and Applications*, Marcel Dekker, New York, 1989.
32. D.A. Cremers, L.J. Radziemski, T.R. Loree, 'Spectrochemical Analysis of Liquids Using the Laser Spark', *Appl. Spectrosc.*, **38**(5), 721–729 (1984).
33. C.W. Ng, W.F. Ho, N.H. Cheung, 'Spectrochemical Analysis of Liquids Using Laser-induced Plasma Emissions: Effect of Laser Wavelength on Plasma Properties', *Appl. Spectrosc.*, **51**(7), 976–983 (1997).
34. J.R. Wachter, D.A. Cremers, 'Determination of Uranium in Solution Using Laser-induced Breakdown Spectroscopy', *Appl. Spectrosc.*, **41**(6), 1042–1048 (1987).
35. D.C. Smith, R.T. Brown, 'Aerosol-induced air Breakdown with $CO_2$ Laser Radiation', *J. Appl. Phys.*, **46**, 1146–1154 (1975).
36. D.A. Cremers, L.J. Radziemski, 'Detection of Chlorine and Fluorine in Air by Laser-induced Breakdown Spectroscopy', *Anal. Chem.*, **55**, 1252–1256 (1983).
37. L.J. Radziemski, T.R. Loree, D.A. Cremers, N.M. Hoffman, 'Time-resolved Laser-induced Breakdown Spectrometry of Aerosols', *Anal. Chem.*, **55**, 1246–1252 (1983).
38. J.A. Aguilera, C. Aragon, J. Campos, 'Determination of Carbon Content in Steel Using Laser-induced Breakdown Spectroscopy', *Appl. Spectrosc.*, **46**(9), 1382–1387 (1992).
39. P.D. Maker, R.W. Terhune, C.M. Savage, *Quantum Electronics (Proc. of Third International Congress, Paris, 1963)*, eds. P. Grivet, N. Bloembergen, Dunod, Paris, and Columbia University Press, New York, 1559, Vol. 2, 1964.
40. R.W. Schmieder, 'Combustion Applications of Laser Induced Breakdown Spectroscopy', Sandia Report SAND81-8886, Sandia National Laboratories, Livermore, CA, 1982.
41. L.J. Radziemski, T.R. Loree, 'Laser-induced Breakdown Spectroscopy: Time Resolved Behavior', LANL Report LA-UR-81-697, Los Alamos National Laboratory, Los Alamos, NM, 1981.
42. L.J. Radziemski, T.R. Loree, D.A. Cremers, N.M. Hoffman, 'Time-resolved Laser-induced Breakdown Spectroscopy (LIBS): A New Method for Spectrochemical Analysis', LANL Report LA-UR-82-487, Los Alamos National Laboratory, Los Alamos, NM, 1982.
43. J. Uebbing, J. Brust, W. Sdorra, F. Leis, K. Niemax, 'Reheating of a Laser-produced Plasma by a Second Pulse Laser', *Appl. Spectrosc.*, **45**(9), 1419–1423 (1991).
44. D.A. Cremers, L.J. Radziemski, 'Direct Detection of Beryllium on Filter Using the Laser Spark', *Appl. Spectrosc.*, **39**(1), 57–63 (1985).
45. K.J. Mason, J.M. Goldberg, 'Production and Initial Characterization of a Laser-induced Plasma in a Pulsed Magnetic Field for Atomic Spectrometry', *Anal. Chem.*, **59**, 1250–1255 (1987).
46. K.J. Mason, J.M. Goldberg, 'Characterization of a Laser Plasma in a Pulsed Magnetic Field. Part I: Spatially Resolved Emission Studies', *Appl. Spectrosc.*, **45**(3), 370–379 (1991).
47. K.J. Mason, J.M. Goldberg, 'Characterization of a Laser Plasma in a Pulsed Magnetic Field. Part II: Time-resolved Emission and Absorption Studies', *Appl. Spectrosc.*, **45**(9), 1444–1455 (1991).
48. D.A. Cremers, 'The Analysis of Metals at a Distance Using Laser-induced Breakdown Spectroscopy', *Appl. Spectrosc.*, **41**(4), 572–579 (1987).
49. D. Bradley, 'News from The Electronic Analytical Chemistry Conference', *Anal. Chem. News & Features*, January 1 (1998).
50. L.W. Peng, W.L. Flower, K.R. Hencken H.A. Johnsen, R.F. Renzi, N.B. French, 'A Laser-based Technique for Continuously Monitoring Metal Emissions From Thermal Treatment Units', *Process Control Quality*, **7**, 39–49 (1995).
51. J.P. Singh, F.Y. Yueh, H. Zhang, R.L. Cook, 'Analytical Method Using Laser-induced Breakdown Spectroscopy', US Patent 5,751,416.
52. B.J. Marquardt, D.N. Stratis, D.A. Cremers, S.M. Angel, 'Novel Probe for Laser-induced Breakdown Spectroscopy and Raman Measurements Using an Imaging Optical Fiber', *Appl. Spectrosc.*, **52**(9), 1148–1153 (1998).
53. W.E. Ernst, D.F. Farson, D.J. Sames, 'Determination of Copper in A533b Steel for the Assessment of Radiation Embrittlement Using Laser-induced Breakdown Spectroscopy', *Appl. Spectrosc.*, **50**(3), 306–309 (1996).
54. B. Flower, H. Johnsen, K. Hencker, D. Hahn, 'Field Test of a Continuous Emissions Monitor for Metals Based on Laser Spark Spectroscopy', Technical report for continuous emission monitor (CEM) test at the Rotary Kiln Incinerator Simulator (RKIS) at the EPA Environmental Research Center, Research Triangle Park, North Carolina, April, 1996.

55. J.P. Singh, H. Zhang, F.Y. Yueh, 'DOE and EPA Continuous Emission Monitoring Test at EPA National Risk Management Research Laboratory (NRMRL)', Technical Report for Continuous Emission Monitor (CEM) Test at the Rotary Kiln Incinerator Simulator (RKIS) at the EPA Environmental Research Center, Research Triangle Park, North Carolina, April, 1996.
56. H. Zhang, F.Y. Yueh, J.P. Singh, 'Laser-induced Breakdown Spectrometry as a Multi-metal Continuous Emission Monitor', *Appl. Optics*, **38**(9), 1459–1466 (1999).
57. H. Zhang, J.P. Singh, F.Y. Yueh, R.L. Cook, 'Laser-induced Breakdown Spectra in a Coal-fired MHD Facility', *Appl. Spectrosc.*, **49**(11), 1617–1623 (1995).
58. D.K. Ottesen, J.C.F. Wang, L.J. Radziemski, 'Real-time Laser Spark Spectroscopy of Particulates in Combustion Environments', *Appl. Spectrosc.*, **43**(6), 967–976 (1989).
59. C.J. Lorenzen, C. Carlhoff, U. Hahn, M. Jogwich, 'Applications of Laser-induced Emission Spectral Analysis for Industrial Process and Quality Control', *J. Anal. At. Spectrom.*, **7**, 1029–1035 (1992).
60. K. Song, Y.I. Lee, J. Sneddon, 'Application of Laser-induced Breakdown Spectroscopy', *Appl. Spectrosc. Rev.*, **32**(3), 183–235 (1997).
61. R.E. Neuhauser, U. Panne, R. Niessner, G.A. Petrucci, P. Vavalli, N. Omenetto, 'On-line and In-situ Detection of Lead Aerosols by Plasma-spectroscopy and Laser-excited Atomic Fluorescence Spectroscopy', *Anal. Chim. Acta*, **346**, 37–48 (1997).
62. J.P. Singh, F.Y. Yueh, H. Zhang, R.L. Cook, 'Study of Laser-induced Breakdown Spectroscopy as a Process Monitor and Control Tool for Hazardous Waste Remediation', *Process Control Quality*, **10**, 247–258 (1997).
63. J.P. Singh, H. Zhang, F.Y. Yueh, K.P. Carney, 'Investigation of the Effects of Atmospheric Conditions on the Quantification of Metal Hydrides Using Laser-induced Breakdown Spectroscopy', *Appl. Spectrosc.*, **50**(6), 764–773 (1996).
64. C. Lazzari, M.D. Rosa, S. Rastelli, A. Ciucci, V. Palleschi, A. Salvetti, 'Detection of Mercury in Air by Time-resolved Laser-induced Breakdown Spectroscopy Technique', *Laser Particle Beams*, **12**, 525–530 (1994).
65. N.B. French, W.J. Haas, P.M. Lemieux, S.J. Priebe, 'Performance Testing of Multi-metal Continuous Emissions Monitors', US EPA, NRMRL, Raleigh, US Department of Energy, EM-Office of Science and Technology, 1998.
66. G.W. Loge, 'A Continuous Calibration Procedure for Reliable LIBS Monitoring of Metals', in *Proceedings of International Conference on Incineration and Thermal Treatment Technologies*, University of California, Irvine, CA, 227–230, 1997.
67. D.W. Hahn, W.L. Flower, K.R. Hencken, 'Discrete Particle Detection and Metal Emission Monitoring Using Laser-induced Breakdown Spectroscopy', *Appl. Spectrosc.*, **51**(12), 1836–1844 (1997).
68. H. Kurniawan, S. Nakajima, J.E. Batubara, M. Marpaung, M. Okamoto, K. Kagawa, 'Laser-induced Shock Wave Plasma in Glass and its Application to Elemental Analysis', *Appl. Spectrosc.*, **49**(8), 1067–1072 (1995).
69. T.L. Thiem, R.H. Salter, J.A. Gardner, Y.I. Lee, J. Sneddon, 'Quantitative Simultaneous Elemental Determinations in Alloys Using Laser-induced Breakdown Spectroscopy (LIBS) in an UltraHigh Vacuum', *Appl. Spectrosc.*, **48**(1), 58–64 (1994).
70. M. Sabsabi, P. Cielo, 'Quantitative Analysis of Aluminum Alloys by Laser-induced Breakdown Spectroscopy and Plasma Characterization', *Appl. Spectrosc.*, **49**(4), 499–507 (1995).
71. C. Argagon, J.A. Aguilera, Campos, 'Determination of Carbon Content in Molten Steel Using Laser-induced Breakdown Spectroscopy', *Appl. Spectrosc.*, **47**(5), 606–608 (1993).
72. L. Paksy, B. Nemet, A. Lengyel, I. Kozma, J. Czekkel, 'Production Control of Metal Alloys by Laser Spectroscopy of the Molten Metals. Part 1. Preliminary Investigations', *Spectrochim. Acta, B*, **51**, 279–290 (1996).
73. K.Y. Yamamoto, D.A. Cremers, M.J. Ferris, L.E. Foster, 'Detection of Metals in the Environment Using a Portable Laser-induced Breakdown Spectroscopy Instrument', *Appl. Spectrosc.*, **50**(2), 222–233 (1996).
74. D.A. Cremers, J.E. Barefield, A.C. Koskelo, 'Remote Elemental Analysis by Laser-induced Breakdown Spectroscopy Using a Fiber-optic Cable', *Appl. Spectrosc.*, **49**(6), 857–860 (1995).
75. A.S. Eppler, D.A. Cremers, D.D. Hickmott, M.J. Ferris, A.C. Koskelo, 'Matrix Effects in the Detection of Pb and Ba in Soils Using Laser-induced Breakdown Spectroscopy', *Appl. Spectrosc.*, **50**(9), 1175–1181 (1996).
76. A.V. Pakhomov, W. Nichols, J. Borysow, 'Laser-induced Breakdown Spectroscopy for Detection of Lead in Concrete', *Appl. Spectrosc.*, **50**(7), 880–884 (1996).
77. S.D. Arnold, D.A. Cremers, 'Rapid Determination of Metal Particles on Air Sampling Filters Using Laser-induced Breakdown Spectroscopy', *AIHA J.*, **56**, 1180–1186 (1995).
78. J.P. Singh, F.Y. Yueh, H. Zhang, K.P. Carney, 'A Preliminary Study of the Determination of Uranium, Plutonium and Neptunium by Laser Induced Breakdown Spectroscopy', *Recent Res. Develop. Appl. Spectrosc.*, **2**, 59–67 (1999).
79. W.E. Ernst, D.F. Farson, D.J. Sames, 'Determination of Copper in A533b Steel for the Assessment of Radiation Embrittlement Using Laser-induced Breakdown Spectroscopy', *Appl. Spectrosc.*, **50**(3), 306–309 (1996).
80. T.L. Thiem, P.J. Wolf, 'Analysis of National Institute of Standards and Technology Ore and United States Geological Survey Samples by Inductively Coupled Plasma Spectroscopy/Laser-induced Breakdown Spectroscopy', *Microchem. J.*, **50**, 244–252 (1994).